8-2012

Multi-Tag Access for a High Precision Ultra-Wideband Localization System

Nathan Carl Rowe
University of Tennessee - Knoxville, nrowe@utk.edu

To the Graduate Council:

I am submitting herewith a thesis written by Nathan Carl Rowe entitled "Multi-Tag Access for a High Precision Ultra-Wideband Localization System." I have examined the final electronic copy of this thesis for form and content and recommend that it be accepted in partial fulfillment of the requirements for the degree of Master of Science, with a major in Electrical Engineering.

Aly Fathy, Major Professor

We have read this thesis and recommend its acceptance:

Paul Crilly, Marshall Pace

Accepted for the Council:
Dixie L. Thompson

Vice Provost and Dean of the Graduate School

(Original signatures are on file with official student records.)

Multi-Tag Access for a High Precision Ultra-Wideband Localization System

A Thesis Presented for

The Master of Science

Degree

The University of Tennessee, Knoxville

Nathan Carl Rowe

August 2012

Acknowledgements

I would like to thank Dr. Aly Fathy for his support and guidance during my graduate studies. His wisdom, experience, and dedication have been invaluable in the preparation of this thesis. He has helped me to overcome many challenges throughout this work, and has continually pushed me to do more and go farther. I would also like to express my gratitude to my committee members Dr. Paul Crilly and Dr. Marshal Pace for their support. Thanks also to my colleagues and supervisors at Oak Ridge National Laboratory for their support of my graduate studies. Finally, I would like to thank my family and friends for their support and encouragement, and especially my parents for continually believing in my abilities.

Abstract

Ultra-Wideband (UWB) wireless positioning systems have many advantages for tracking and locating items in indoor environments. Surgical navigation and industrial process control are potential applications for high accuracy UWB localization systems with millimeter or sub-millimeter accuracy. I present improvements made to an existing high accuracy, multi-tag, UWB localization system. The goal of this thesis was to improve the multi-tag performance of this system while maintaining the high localization accuracy, and to utilize the UWB system for digital communications allowing the existing narrowband 2.4 GHz transceiver to be eliminated.

This thesis presents a proof-of-concept for a multi-tag, UWB localization system utilizing orthogonal time hopping multiple access (OTHMA). Asynchronous transmit-only UWB digital communication allows identification of tags without the use of a narrowband control channel, and time difference of arrival (TDOA) accomplishes localization. A digital sampling circuit is used for both localization and digital communication. I address the inherent challenge of collisions in an asynchronous transmit-only system while maintaining high accuracy and high update rates. An experimental system was developed consisting of two base stations and two tags allowing measurement of 1-D localization accuracy along with system update rates. The experimental results for localization accuracy were equivalent to results from the existing system while update rates were improved by greater than 50%.

Contents

List of Tables

List of Figures

Chapter 1

Introduction

1.1 Motivation

There are many potential uses for a high accuracy localization system that can track a tag position with millimeter or better accuracy. The University of Tennessee has developed an ultra-wideband (UWB) localization system designed with a focus on biomedical applications, particularly surgical navigation. The system and research could also be applied to many fields requiring high accuracy positioning such as industrial process control or high value asset tracking. In almost all applications the need exists to track multiple objects or multiple points on these objects nearly simultaneously. This is the motivation for developing methods of multiple access for these systems.

1.2 Overview

This thesis presents research and development into improving UWB multi-tag performance specifically in the context of a high accuracy localization system. The multi-tag scheme that has been developed is directly applicable to UT's UWB localization system and in the future may serve to replace the existing system which is based on a low power 2.4GHz control channel. As such the scheme is partly

based on the unique constraints and available hardware for this system, but could be generalized for use in other UWB localization systems. The goal of this research is to improve the multi-tag performance by reducing the localization time required for individual tags and eliminating the need for a currently used narrowband 2.4GHz transceiver by utilizing the UWB system for digital communications as well. These goals should be met without significantly limiting the localization accuracy of the system.

The design of a UWB digital communications system, while challenging on its own, is well understood and many methods have already been investigated and documented. This work is significant because it incorporates both digital communication and a high accuracy localization system based on sub-sampling into a common platform. The methods developed here take advantage of common hardware to accomplish both tasks and limit the need for additional communications specific hardware. Development challenges and design trade-offs are described in Chapters 3 and 4.

1.3 Contributions

This work is based on prior work into UWB high accuracy localization systems done at the University of Tennessee beginning with Drs. Cemin Zhang and Brandon Merkl who graduated in 2008, Dr. Depeng Yang who graduated in 2011, Michael Kuhn who graduated in 2012, and the current team including Jonathan Turnmire and Essam Elkhouly. This work also takes advantage of a digital sampling circuit originally designed for a UWB see-through-walls radar system by Drs. Yazhou Wang and Quanhua Liu. The material presented in this thesis is only possible because of the contributions of this entire team. Within this context, my individual contributions are in the area of multi-tag access and related system modifications. These contributions include:

- Integration of an FPGA based digital sampler to replace the existing analog sub-sampler. The digital sampler was required to implement the desired digital communications scheme, but also has advantages for the speed and accuracy of sub-sampling. The digital sampling board was originally designed for use with a see-through walls radar system [8]. A significant modification to the FPGA program was required to allow processing of pulse time of arrival from sub-sampled signals in the FPGA in real-time rather than post-processing as done previously. This modification allows a higher rate of reception by minimizing processing time between sub-sampling periods.

- Design and implementation of a digital communications scheme based on on-off keying (OOK) of UWB pulses. This scheme requires a digital sampler that can synchronize sampling with received pulses. Implementation of the digital communication scheme required the addition of functionality to the FPGA program running on the digital sampler. A separate FPGA program was also developed as a tag controller to generate the digital signal for the required transmission sequence.

- Implementation of a multi-tag high accuracy localization system based on the digital communications scheme. The system utilizes a common transmitter and receiver along with the digital sampler circuit for both localization and digital communication. The complete system uses microwave circuit components from the previous system including the UWB transmitter, front-end, and non-coherent receiver. This system eliminates the need for a narrow band control channel, allows for faster refresh rates of individual tags, and simplifies the tag architecture which may provide benefits to battery life and production costs.

- Experimental analysis of the multi-tag system. The analysis included two base stations and two tags allowing evaluation of the update rate of the system and the 1-dimensional localization accuracy. The results provide update rate

and accuracy measures, and a comparable experiment was conducted with the existing UT system allowing direct comparison.

1.4 Organization

The thesis begins in Chapter 2 with a discussion of background and prior related work. Then a criteria for comparing performance is introduced in Chapter 3 and performance trade-offs are investigated. A theoretical limitation for expected system performance is also developed for both this work and the prior existing system. Chapter 4 describes the implementation of a multi-tag high accuracy localization system based on the multi-tag scheme that was developed. Then Chapter 5 describes the experimental analysis of this system. Finally Chapter 6 describes potential next steps in advancing this system and Chapter 7 recaps the advantages of moving to this new multi-tag scheme and the significance of the experimental results.

Chapter 2

Background & Prior Research

2.1 Ultra-Wideband Localization Overview

UWB is commonly defined as a wireless technology utilizing narrow pulses, resulting in very wide bandwidth, to transmit data. The Federal Communications Commission (FCC) defines UWB as any transmission which occupies greater than 20% fractional bandwidth or greater than 500MHz total bandwidth [9]. Figure 2.1 demonstrates the relationship between UWB and narrowband signals in both the time domain and frequency domain. In general the bandwidth of a UWB signal is inversely proportional to the pulse width. Pulse widths are typically on the order of 1ns or less with resulting bandwidths greater than 1GHz.

The technology's strengths include robust performance in challenging multi-path environments, potential for high data rates, and the ability to share bandwidth with traditional narrowband signals. The narrow pulse transmissions also provide an advantage in localization. Systems using time difference of arrival (TDOA) take advantage of the narrow pulses to accurately measure the time of arrival at multiple base stations. By taking the difference in arrival time at the receivers the position of a tag can be triangulated.

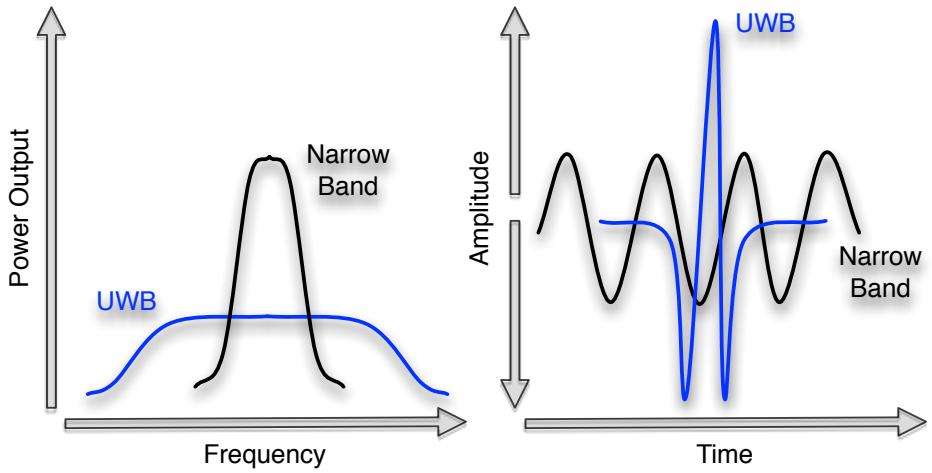

Figure 2.1: Comparison of UWB to narrow band in the time domain and frequency domain.

Localization systems typically utilize one of two common topologies: remote positioning or self-positioning depending on whether the location is computed on the mobile tag or in a fixed base station. Either of these topologies has an indirect form in which the location is transmitted back to the other unit for use there [10]. The UT system utilizes a remote positioning topology as seen in figure 2.2. Multiple tags operate as mobile transmitters whose positions can be localized. The base stations operate as stationary receivers and typically serve as fixed points of reference for localization. The received signal from multiple base stations is combined to compute the location of the tag using TDOA.

2.2 IEEE 802.15.4 Standard

The IEEE 802.15 working group maintains the IEEE 802.15.4 standard for low-rate wireless personal area networks (LR-WPANs) to which a specification for a UWB physical layer (PHY) was added in 2007. It is designed to provide LR-WPAN devices that are low cost, low power, robust to multipath fading, and able to support precise ranging [11]. The task group considered a number of multi-tag

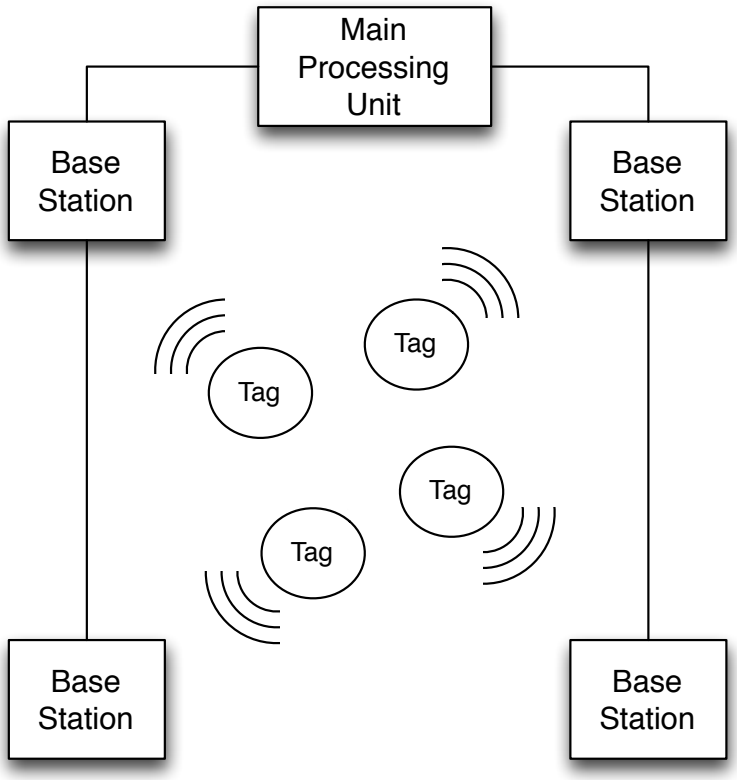

Figure 2.2: Remote positioning topology with mobile transmitters, referred to as tags, and fixed receivers, referred to as base stations.

access methods for possible inclusion in the standard. Possible modulation techniques include pulse position modulation (PPM), On-Off Keying (OOK), binary phase shift keying (BPSK), and burst position modulation (BPM) [7]. The 802.15.4a task group selected a combination of burst position modulation (BPM) and binary phase shift keying (BPSK) for the signaling scheme because of its applicability to both coherent and non-coherent receiver approaches and its advantages in bit-error-rate (BER). An optional chaotic on-off keying (COOK) modulation technique was also included for its advantages in low-power applications [11].

2.3 State-of-the-Art in UWB Localization

Several commercial UWB positioning systems currently exist and more are in development. Many of the systems use proprietary technology, but some newer systems under development are based on the IEEE 802.15.4a standard. Details of several UWB localization products are provided in table 2.1.

Table 2.1: Comparison of commercial UWB localization systems. [1, 2, 3, 4, 5]

Company	Product	Frequency Range (GHz)	Operating Range (m)	Localization Accuracy (mm)
Zebra	Sapphire Dart	6.35 - 6.75	100	300
Ubisense	RTLS	5.8 - 7.2	50	150
Time Domain	Pulson 400	3.1 - 5.3	354	70
Decawave	ScenSor1	3.5-6.5	70	100

Sapphire Dart by Zebra Technologies and the Real Time Location System (RTLS) by Ubisense are two UWB localization products providing precise asset tracking capabilities. The Zebra and Ubisense systems can be seen in Figure 2.3. They both use proprietary methods for localization and multi-access rather than conforming to the IEEE 802.15.4a standard. The Zebra system uses TDOA to determine tag location and pulse modulation for digital communication. The Ubisense system uses both TDOA and Angle of Arrival (AOA) together to determine tag location. It doesn't use the UWB radio for digital communication, but instead uses a narrowband channel selectable from 902-928MHz, 433-434MHz, or 869-870MHz. Both systems have a range of greater than 100m, and an accuracy better than 30cm for tag localization.

The Pulson 400 by Time Domain provides a UWB OEM Module for ranging and communications. It can be seen in Figure 2.4a. The Time Domain system uses proprietary methods for UWB data communication and ranging. The system uses precise time-of-flight (TOF) measurements between modules for ranging. The modules don't use a remote positioning system topology by default, but could be arranged in this architecture for localization. The system can support data

(a) (b)

Figure 2.3: Two commercial UWB localization systems: (a) Sapphire Dart by Zebra Technologies and (b) RTLS by Ubisense. [1, 2]

communication at rates up to 158kbps. The UWB module is available in a 3 inch by 4 inch package for inclusion in custom designed systems.

The ScenSor1 by Decawave, seen in Figure 2.4b, is an upcoming radio communications chip based on the IEEE 802.15.4a specification. It functions as both a UWB transmitter and receiver also providing ranging capabilities for localization. The chip supports ranging using TOF based on the IEEE specification. A remote positioning system topology is not required, but could be used. The data communication uses binary phase shift keying (BPSK) with binary position modulation (BPM). The entire transceiver is integrated in a CMOS silicon wafer technology 4.5 x 4.5mm 64 pin BGA package. Table 2.2 compares the performance of these commercial systems in number of tags, refresh rate, and localization accuracy.

2.4 UT 2nd Generation Localization System

The UT high accuracy localization system development began in 2008 with development of what would become the 1st generation positioning system. Since then a 2nd generation of the system has been developed to include the capability for real-time dynamic tracking of multiple tags. The second generation system also improves on

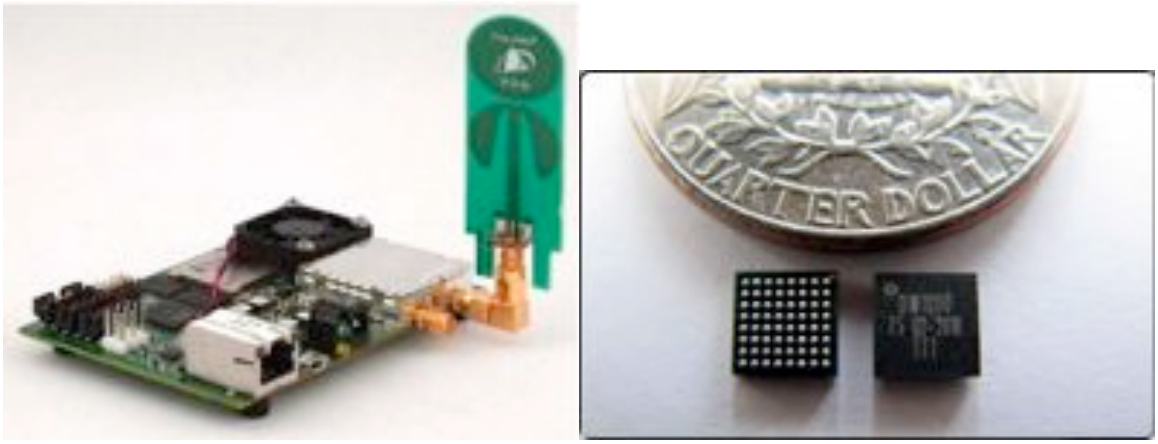

(a) (b)

Figure 2.4: Two commercial UWB development packages including support for localization: (a) Pulson 400 by Time Domain and (b) ScenSor1 by Decawave. [4, 5]

Table 2.2: Comparison of multi-tag access in UWB localization systems. [1, 5, 6]

Company	Refresh Rate (Hz)	Max Tags	Localization Accuracy (mm)
Zebra	1	3500	300
Ubisense	134	1	150
Time Domain	40	7	70
Decawave	1	11000	100
UT	20	30	2-3

the first in dynamic accuracy and overall system stability by including support for an additional base station and adaptable ranging algorithms based on signal-to-noise ratio. The second generation system, described briefly here, serves as the basis for this work providing context and a point of comparison. Both 1st and 2nd generation systems are described in detail in [7].

As described in section 2.1, the UT system utilizes a remote positioning topology with mobile tags, fixed base stations, and a main processing unit. The second generation system includes 10 integrated mobile tags and 5 base stations. Tags act as UWB transmitters producing narrow pulses upconverted to 8GHz. Localization is based on the TDOA of these pulses at the base stations. Figure 2.5 provides an

example of acquiring TDOA measurements. Localization based on TDOA requires a minimum of $n+1$ base stations where n is the number of dimensions to be resolved. For 3-dimensional localization a minimum of 4 base stations is required. The second generation system integrates a 5th base station which provides redundancy in cases where one base station has a poor signal-to-noise ratio. The 5th base station also provides an advantage in geometric dilution-of-precision. A more complete description of geometric dilution-of-precision and the advantages of additional base stations can be found in [7].

The second generation tags are an integrated design shown in Figure 2.6 and associated block diagram in Figure 2.7. The design is divided into two circuit boards: an RF board and a power board. It utilizes a step recovery diode (SRD) based pulse generator, designed at UT, capable of generating 300 ps full-width half max pulses with greater than 3 GHz bandwidth. [12] The pulse generator is triggered by a 10 MHz clipped sine wave from a Vectron VTC4-A0AA10M000 crystal with an op-amp based current amplifier. The crystal has a low phase noise of 1-1.5 ps RMS jitter and high frequency stability of ± 0.5 ppm. A Hittite H506 voltage controlled oscillator produces an 8 GHz local oscillator signal that is mixed with the pulses using a Hittite H553 mixer. The resulting unconverted signal is amplified by a Hittite H441 medium power amplifier before transmission from a monopole antenna.

The transmitted UWB signal is received at the base stations via a directional Vivaldi antenna. The received signal is bandpass filtered from 5-11 GHz to limit out-of-band interference. The second generation base stations utilize one of two different receiver front-ends: a discrete design or an integrated MMIC chip based receiver. The receiver front-ends can be compared in the block diagram in Figure 2.8. Both utilize a non-coherent squaring demodulation approach. The resulting baseband signal, with approximately 3 GHz bandwidth, is passed to an analog sampling mixer. The analog sampling mixer sub-samples a received pulse train at 9.996 GHz providing a time expansion factor of 2,500. The sampling mixer provides some amplification and filtering resulting in a smoothed equivalent signal at 4kHz. This sub-sampling

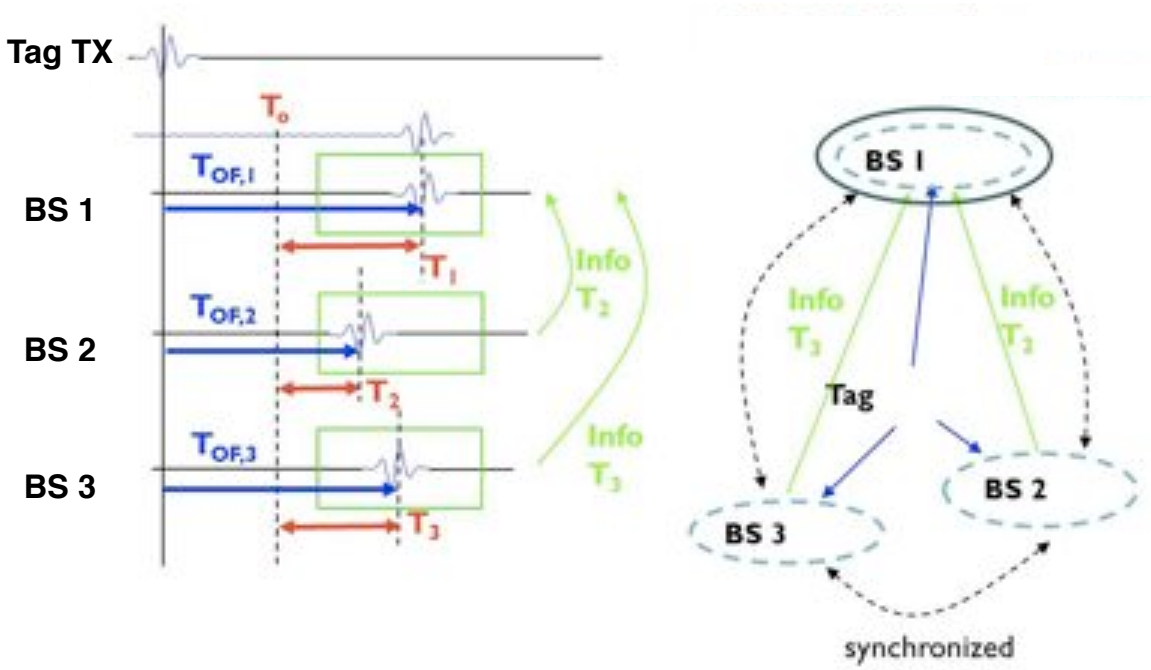

Figure 2.5: TDOA measurements T_1, T_2, and T_3 (left) are used to calculate differences in distances to multiple base stations (right).

approach allows for signal sampling resolution equivalent to 40 ps while utilizing a low cost ADC.

The sub-sampled baseband signals from each base station are passed to a main processing unit for analog-to-digital conversion and TDOA measurement. An Analog Devices AD9216 ADC digitizes the incoming signal at 50MHz for processing in an FPGA. Four Xilinx Spartan 3 FPGAs are utilized in the configuration shown in Figure 2.9. Three of the FPGAs process received signals as shown in Figure 2.10 to detect the leading edge of received pulses and calculate the signal-to-noise ratio. The final FPGA is utilized as a control station that integrates the resulting leading edge measurements to calculate TDOA. The resulting TDOA measurements are sent to a host PC for data collection and visualization.

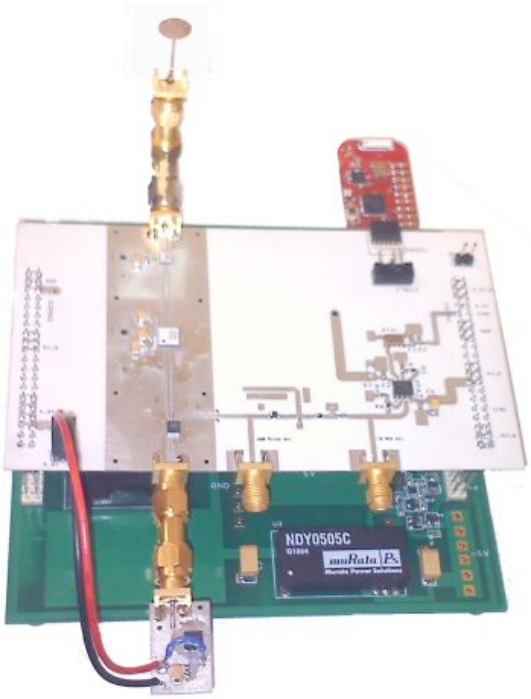

Figure 2.6: The existing integrated tag design using an MSP430-RF2500 development board for tag control. [7]

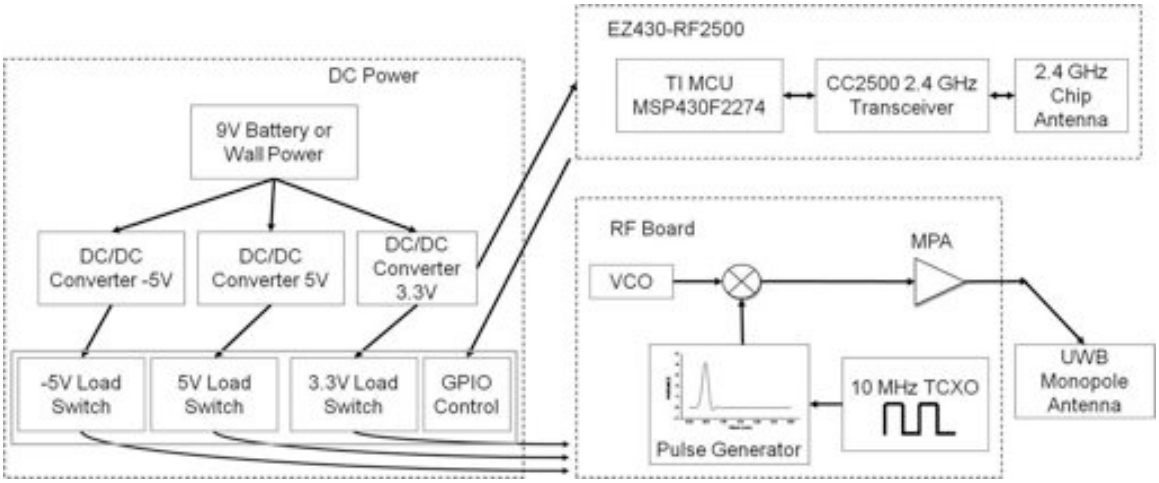

Figure 2.7: Block diagram of the second generation system integrated tag. [7]

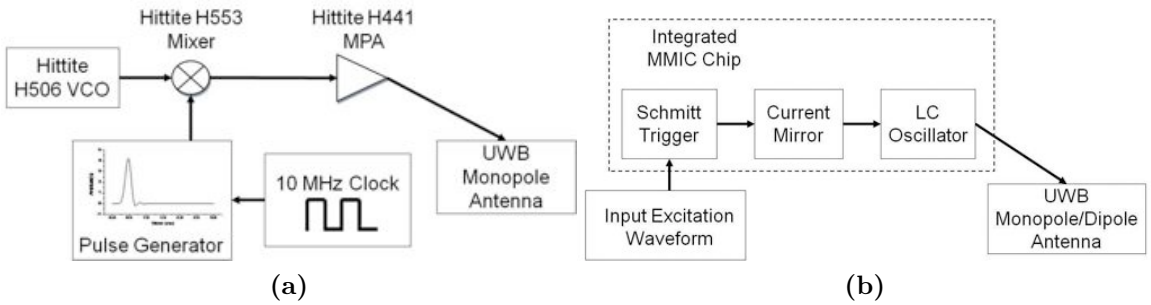

Figure 2.8: Two different receiver front-ends can be used: (a) Discrete and (b) MMIC. [7]

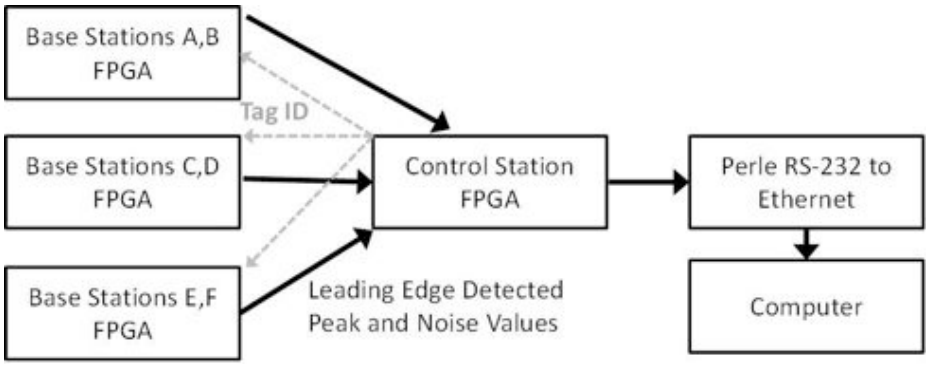

Figure 2.9: Block diagram of the main processing unit showing the connection of the 4 FPGAs used for signal processing and computer interface. [7]

2.5 2nd Generation System Multi-Tag Access

A number of possible methods for multi-tag access were considered in the development of the UT system. Some of the options considered include Wi-Fi 802.11b, Bluetooth, 802.15.4f UWB either BSPK or OOK modulation, 802.15.4f 2.4GHz, and Zigbee. It was decided that UWB OOK was the preferred choice for many reasons including battery life, simplified transmitter and receiver architectures, and operation without the need for accurate channel estimation. [7] Even though this was recognized as the preferred solution at the time, the system that was finally implemented was based on an off-the-shelf 2.4 GHz transceiver also compatible with 802.15.4f. This technology was selected because of its maturity and the ready availability of low cost development tools. In contrast, low power UWB OOK transceivers are still an immature technology

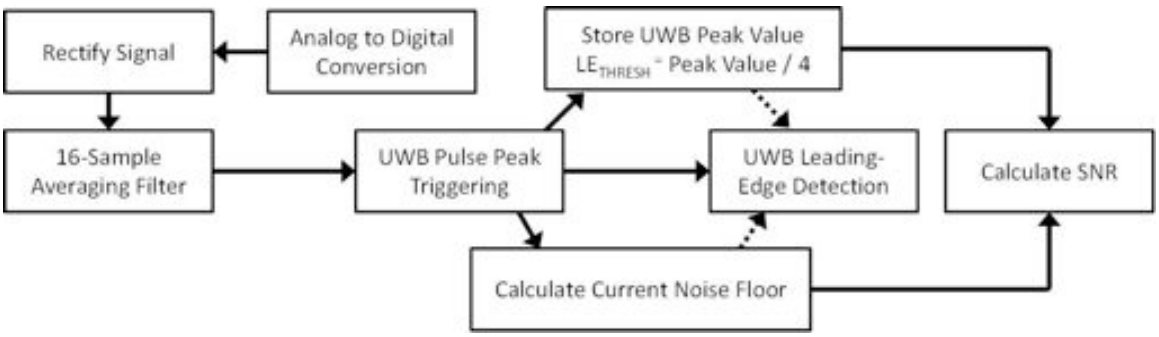

Figure 2.10: Digital signal processing that occurs in the base station FPGAs. [7]

with few industry adopters and significant research ongoing. Most significantly low power CMOS implemented transceivers are not for sale commercially.

The multi-tag system that was finally developed at UT is based on an MSP430-RF2500 combination micro-controller unit (MCU) and 2.4GHz transceiver. The MCU controls MOSFET integrated load switches that switch power on and off to the UWB transmitter. The switching of tags is organized from a CPU using another MSP430-RF2500 module, called the access point MCU, which implements a simple TDMA round-robin scheme for multi-tag access. The control station FPGA's in the main processing unit are connected to the access point via two lines for digital communication. The access point transmits asynchronously each tag ID as it becomes active. The FPGA then labels incoming TDOA measurements using the current tag ID and transmits this along with TDOA measurements to the host PC.

2.6 2nd Generation System Results

A summary of experiments from both the 1st and 2nd generation systems are provided in Table 2.3. Most of the experiments were conducted with 4 or more base stations providing 3-D dynamic tracking results, but a limited set of 1-D results is also provided. Dynamic experiments involve actively moving tags by freeform hand movement, movement along an optical rail, or by pre-programmed robotic arm. All accuracy results are given as root mean square (RMS) error since values are

expected to fluctuate above and below the true location, and multi-tag performance is expressed in events per second as described in the following chapter 3.2. For the 2nd generation system 3-D accuracy ranges from 9.54mm in regular tracking mode to as low as 3.26mm in high accuracy tracking mode with 5 base stations, and 1-D accuracy ranges from 2.52mm to 0.93mm for high accuracy tracking mode with 5 base stations. The multi-tag performance is based on 10 tag experiments in which the maximum update rate was 15Hz for regular tracking mode and only 8Hz for high accuracy tracking mode.

Table 2.3: Experimental results for both 1st and 2nd generation UT localization systems. [7]

Experiment	RMS Error (mm)	
1st Generation System		
3-D Dynamic Freeform	6.37	N/A
3-D Dynamic Robot	5.24	N/A
3-D Static (20 Locations)	4.67	N/A
3-D Static w/ 106 sample averaging	1.98	N/A
2nd Generation System		
3-D Dynamic Freeform		
(Regular Tracking Mode)	9.54	1000
(High Accuracy Tracking Mode)	6.71	1000
3-D Dynamic Optical Rail		
(5 Base Stations)	3.26	1000
1-D Dynamic Optical Rail		
X-Direction	2.52	1000
Y-Direction	0.93	1000
Z-Direction	1.83	1000

This multi-tag scheme utilized in the 2nd generation system has advantages and disadvantages as outlined in table 2.4. These factors will effect its appropriateness for any given application. Primary advantages are the availability of mature proven 2.4GHz transceivers, ability to control tags during operation for adjustment of refresh rate, and flexibility for using analog or digital sub-sampling techniques. The primary disadvantage is the need for an additional non-UWB transceiver. This additional hardware will increase tag size, cost, and power requirements. More importantly,

reliance on a narrowband channel limits the advantage of UWB strengths such as robust performance in challenging multi-path environments, potential for high data rates, and the ability to share bandwidth with traditional narrowband signals. Secondarily, this scheme is limited in the potential for future improvements due to the fundamental performance of the commercial off-the-shelf transceiver.

Table 2.4: Advantages and disadvantages of the 2nd generation system 2.4GHz based multi-tag access approach

Advantages
Wireless Tag Control
Synchronized tag transmission eliminates inter-tag interference
Commercially available development tools
Disadvantages
Requires a 2.4 GHz transceiver for each tag
Higher tag cost, increased power consumption, and complexity
Both UWB and Narrow Band signals

Chapter 3

Multi-Tag Access Theory

3.1 Overview

Multi-tag access is a fundamental requirement for almost all localizations systems. The system design must address two primary requirements of a multi-tag system. First, tags must provide some unique signature or signal that allows the system to identify them and separate their transmissions from other tags operating in the same area. This is commonly accomplished using digital communications allowing the tag to report some unique ID number. Second, the system must address the potential for interference between two or more tags transmitting in the same area. This is accomplished using a multiple access method, where some form of either Time Division Multiple Access (TDMA), Code Division Multiple Access (CDMA), or Frequency Division Multiple Access (FDMA) is used. Since the UWB localization system makes use of time domain information, multi-tag systems will generally be required to operate without disrupting the time series information. For this reason, schemes utilizing TDMA are typically preferred and in this chapter we will restrict our discussion to the TDMA case. Many of the commercial systems and the 2nd generation UT system described in chapter 2 utilize this approach to multiple access.

This chapter begins by introducing a set of performance metrics for a multi-tag localization system that allows comparison of a system based on accuracy, number of tags vs. update rate, and ability to track a moving object. Then a theoretical analysis of an ideal multi-tag system is presented in order to provide an upper bound on achievable performance, investigate the effect of localization parameters on multi-tag performance, and finally to demonstrate the theoretical trade-off between accuracy and multi-tag performance. Next, a synchronous approach to multi-tag access like that of the 2nd generation UT system, is investigated along with the limitations it places on system performance. Finally, an asynchronous multi-tag approach, as used in this work, is presented with its advantages and disadvantages. The theoretical limits of its performance are developed and compared with both the 2nd generation UT system and the ideal system.

3.2 Performance Metrics

In investigating multi-tag performance for localization systems it is important to define performance criteria that can be used in analyzing these systems. System performance criteria include the accuracy of the system, number of tags, and refresh rate. Accuracy is typically expressed as the root-mean-square (RMS) error in position, typically millimeters (mm) in this work. For multi-tag performance, it is convenient to combine the number of tags and refresh rate into one measure, which will be referred to as events per second. In the ideal case, the number of tags, K, and refresh rate, R, scale inversely so that when multiplied together they provide a figure of merit constant "events per second", (EPS), as seen in equation (3.1).

$$(EPS) = K * R \tag{3.1}$$

While this is a useful measure of multi-tag performance, it may not provide a complete picture of system operation when some form of low pass filtering, typically

a form of simple running average filter, is used on the raw localization numbers to provide better accuracy. This form of filter may limit the ability to track fast moving objects dynamically. For this reason, we also introduce two other measures of system accuracy for dynamic tracking: location uncertainty vs. speed and frequency response. Location uncertainty versus speed is a measure of the accuracy error that results from the time between system refreshes of tag location combined with the effect of filtering based on tag speed. The frequency response simply provides a measure of the systems ability to track a tag moving with periodic motion of a given frequency. The application of these measures to this thesis is limited since proof-of-concept testing has been limited to static tag localization. Applications of dynamic testing of this system is discussed in chapter 6 on Next Steps.

3.3 Ideal System

In order to understand performance trade-offs and generalize performance metrics, it is useful to first understand the ideal case of a multi-tag system using TDMA. In this ideal case, we consider the tags to operate with perfect synchronization requiring no delay between tags and no time required for tag identification. The ideal case is limited only by the time required for each tag to be localized. The organization of this ideal TDMA system can be seen in Figure 3.1. The term packet will be used to describe the tag transmission sequence required for the system to provide a single location measurement. The term frame, as seen in the figure, is used to describe the time period in which all tags transmit a single packet. The length of a frame, T_f, is defined as the inverse of the transmit rate of the tags. Frames can be further divided into slots each of which is sized to fit a single packet. The boundaries of the frame are arbitrary, and for convenience we always define the frame to begin at a slot or packet boundary. In the ideal system, each frame contains precisely the number of slots required to operate all tags, and since in the ideal case all transmissions are

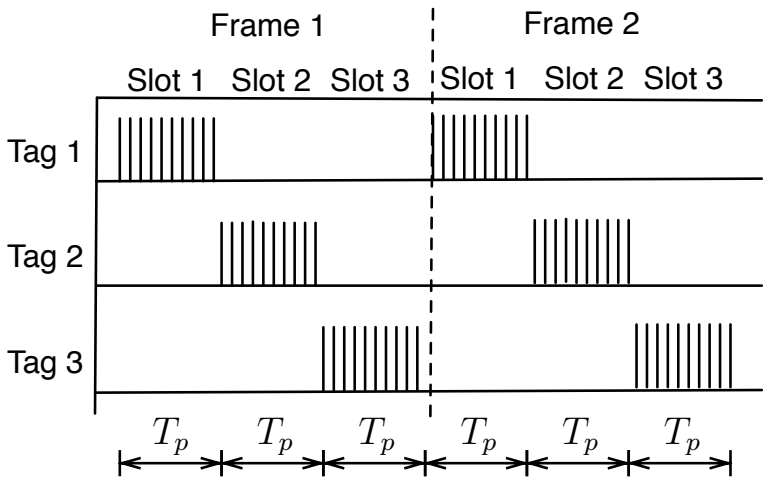

Figure 3.1: Diagram of an ideal multi-tag system showing packets organized in perfect TDMA.

successful the refresh rate is equivalent to the transmit rate. Thus the number of tags supported scales inversely with the refresh rate as described in (3.2).

$$K * T_p = T_f = \frac{1}{R} \tag{3.2}$$

Constant T_p is the packet duration, and is the only parameter in the ideal case. It defines the scale of the relationship between the refresh rate, R, and number of tags, K. The packet duration, T_p, is defined by the time required to localize and identify any individual tag. The limitations on packet duration are discussed in the next section. The relationship between number of tags supported and refresh rate for various packet durations can be seen in Figure 3.2. Solving (3.2) for the performance metric of events per second described in the previous chapter yields (3.3).

$$(EPS) = \frac{1}{T_p} \tag{3.3}$$

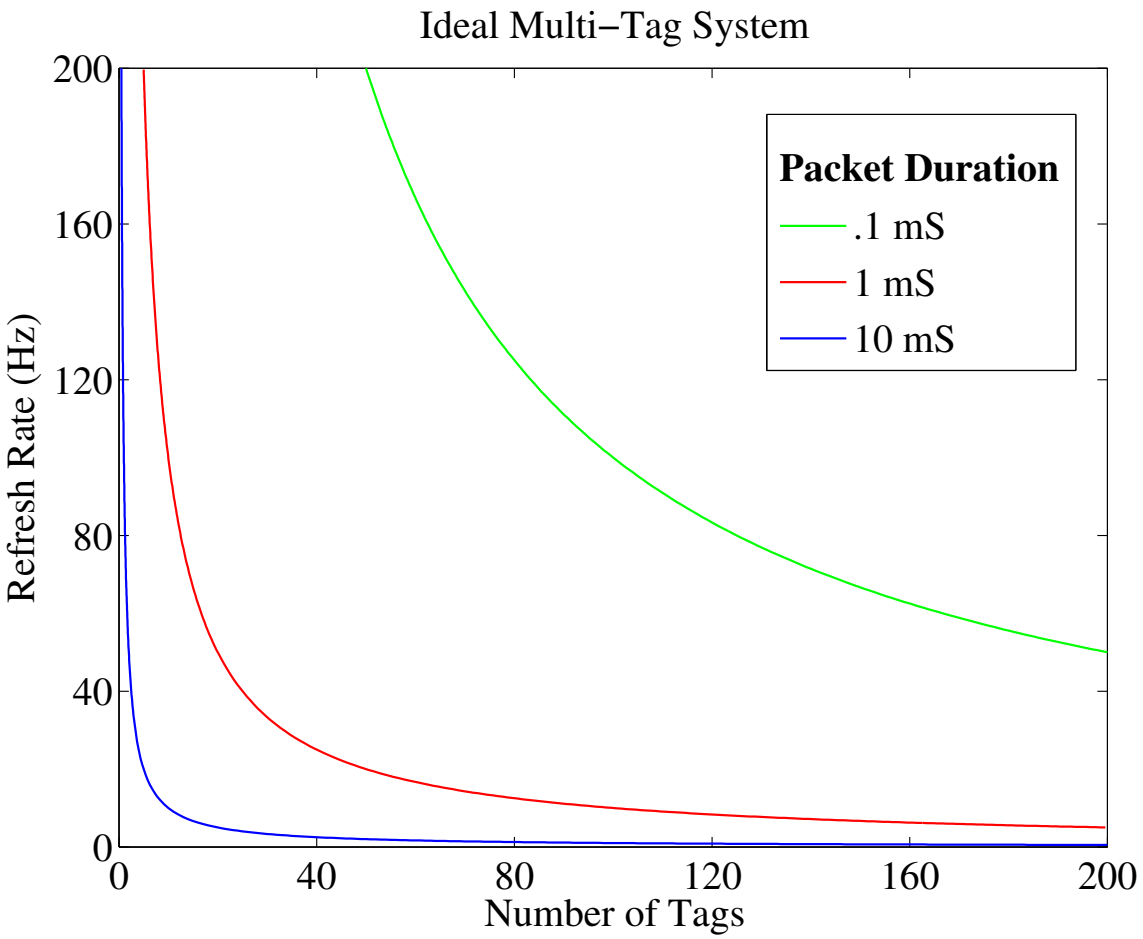

Figure 3.2: Number of Tags vs. Refresh Rate in the Ideal TDMA System.

So as the packet duration decreases the multi-tag performance increases, and as packet duration increases the multi-tag performance decreases. This can be seen in Figure 3.3 along with the results for the packet durations from both the 2nd generation system and this work .

3.4 Localization Constraints

As seen in the ideal case, the packet duration sets a constraint on the maximum achievable multi-tag performance (i.e. tag numbers and refresh rates). In the UT system, the packet duration is limited by the use of sub-sampling, also called

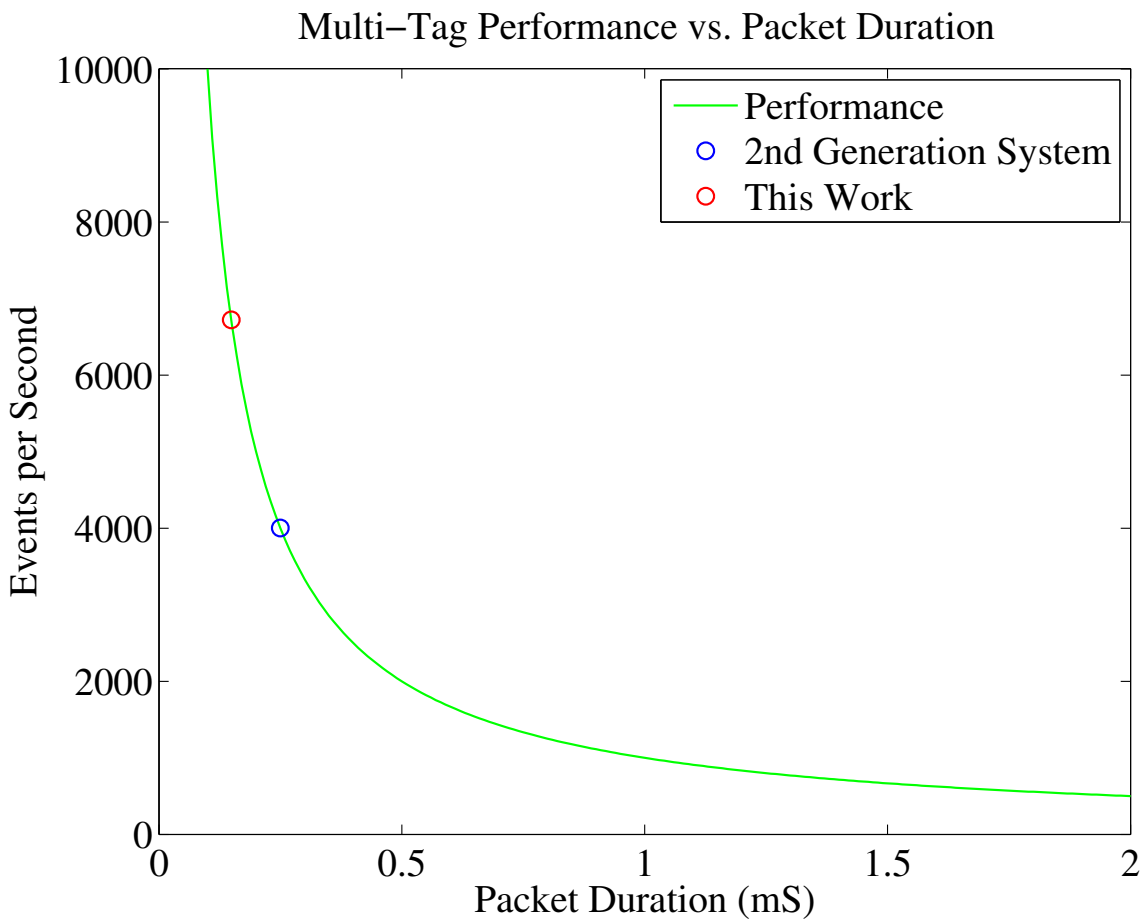

Figure 3.3: Effect of packet duration on multi-tag performance in the ideal multi-tag case.

equivalent time sampling, to make accurate time difference of arrival (TDOA) measurements. Sub-sampling is used to achieve very high equivalent sampling rates with much lower cost electronics than is possible with real-time analog-to-digital converters. Two main parameters affect packet duration: expansion factor, e, and sampling rate, f_s. How these factors affect the packet duration can be seen in (3.4).

$$T_p = \frac{e}{f_s} \tag{3.4}$$

These factors will constrain the maximum multi-tag performance of the UT system. By substituting (3.4) into (3.3) for T_p yields (3.5) which shows the effect of these parameter on the multi-tag performance.

$$(EPS) = \frac{1}{T_p} = \frac{f_s}{e} \tag{3.5}$$

As an example, the 2nd generation system utilizes an expansion factor of 12500 and a sampling rate of 50MHz. As seen in (3.6), these parameters require a packet duration of at least 250μS for each localization which limits the multi-tag performance to a maximum of 4000 events per second as seen in (3.7). This work utilizes an expansion factor of 11160, an average sampling rate of 75MHz, and no TDOA averaging. As seen in (3.8), these parameters require a packet duration of at least 149μS for each localization which limits the multi-tag performance to a maximum of 6720 events per second as seen in (3.9). These numbers are for an idealized multi-tag system that is limited only by the requirements of localization. Actual performance results are much lower due to additional constraints imposed by the multi-tag access method and available hardware performance.

$$T_p = \frac{12500}{50MHz} = 250\mu S \tag{3.6}$$

$$(EPS) = \frac{1}{250\mu S} = 4000 \tag{3.7}$$

$$T_p = \frac{11160}{75MHz} = 149\mu S \tag{3.8}$$

$$(EPS) = \frac{1}{149\mu S} = 6711 \tag{3.9}$$

3.5 Trade-offs with Localization Accuracy

Since the expansion factor has a direct impact on the multi-tag performance and it also directly impacts the equivalent time resolution of the sub-sampling, it contributes to a trade-off between multi-tag performance and localization accuracy. For a system utilizing sub-sampling, the time resolution, t_{res}, between individual samples is set by the repetition frequency, f_{rep}, of the signal to be sub-sampled and the expansion factor, e, used as seen in equation (3.10). The positional resolution, p_{res}, of the tag location as measured by TDOA is then calculated as seen in equation (3.11) to be one half the sample time resolution, t_{res}, multiplied by the speed of light, c. We can then solve for the relationship between the mutli-tag figure of merit, events per second, and the position resolution as seen in (3.12). The multi-tag performance is linearly related to the position resolution and therefore inversely related to the localization accuracy. As multi-tag performance increases, the position resolution also increases resulting in worse localization accuracy. The position accuracy as calculated here sets a limit on the best achievable accuracy of individual localization measurements. While this has a direct impact on the localization accuracy of the system, final results can be slightly better or worse depending on other factors including the averaging that is applied over a sample window, and the distribution of individual localization measurements.

$$t_{res} = \frac{1}{f_{rep} * e} \tag{3.10}$$

$$p_{res} = \frac{t_{res} * c}{2} = \frac{c}{2 * f_{rep} * e} \tag{3.11}$$

$$p_{res} = \frac{c * (EPS)}{2 * f_{rep} * f_s} \tag{3.12}$$

As an example, the 2nd generation system uses a pulse repetition frequency of 10 MHz and a sampling frequency of 50 MHz. As seen in equation (3.13), these parameters result in a position resolution of $1.5\mu m * s$ for each event per second of multi-tag performance. For this thesis a pulse repetition frequency of 10MHz and an equivalent sampling frequency of 75 MHz were used. As seen in equation (3.14), these parameters result in a better position resolution of $0.2\mu m * s$ for each event per second of multi-tag performance. Figure 3.4 demonstrates the position resolution to events per second trade-off for both systems. The expansion factor chosen for each system result in similar position resolutions, but more than 50% improvement in the multi-tag performance for this thesis over the 2nd generation system.

$$p_{res} = \frac{c * (EPS)}{2 * 10MHz * 50MHz} = 0.3x10^{-6} * (EPS) \tag{3.13}$$

$$p_{res} = \frac{t_{res} * c}{2} = \frac{c * (EPS)}{2 * 10MHz * 75MHz} = 0.2x10^{-6} * (EPS) \tag{3.14}$$

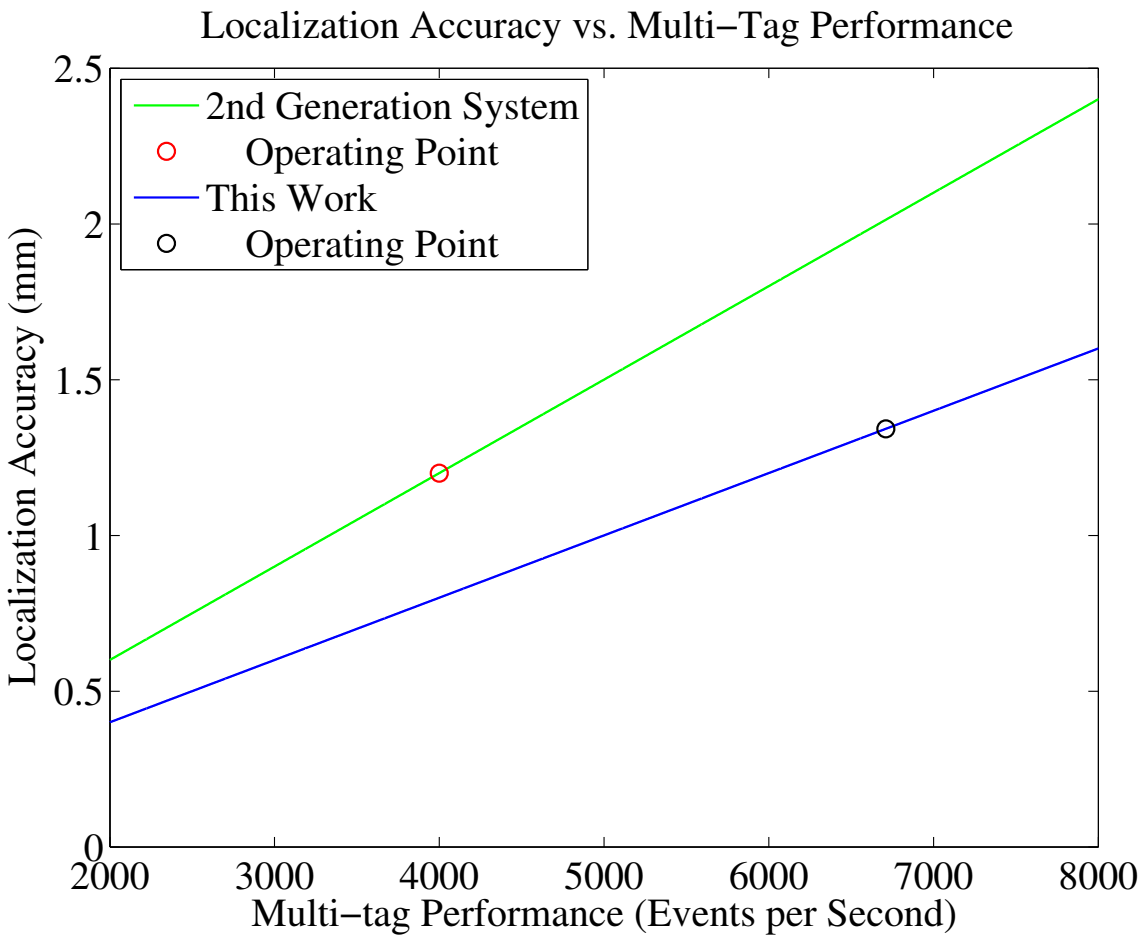

Figure 3.4: Trade-off between localization accuracy and multi-tag performance as set by the expansion factor used for sub-sampling.

3.6 Synchronous Multiple-Access Constraints

The multi-tag performance is also constrained by the performance of the multiple-access scheme. In a synchronous multiple-access scheme tags have a central control station that organizes their packets in a round-robin fashion using a 2.4GHz transceiver.[7] In a perfect system the tags would be able to transmit immediately after each other allowing performance to approach the ideal case, but in reality control speed and accuracy are limited requiring a switching delay, or guard time, to be applied between tag transmissions. Figure 3.5 shows the synchronous system and the

guard time. The switching delay between tags reduces the performance by adding a time delay to each localization. The switching delay is represented by T_d in (3.15).

$$(\text{EPS}) = \frac{1}{T_p + T_d} \tag{3.15}$$

The 2nd generation UT system utilized a synchronous multiple-access scheme controlled via a 2.4GHz communication channel as discussed in chapter 2. The switching delay of this system is estimated to be 25μS per packet. As seen in (3.16), this switching delay reduces the maximum events per second from 4000 in the ideal case to 3636. Actual performance described in chapter 2 is limited by the data transfer capability of the FPGA serial connection to the computer resulting in the lower performance of only 1000 events per second.

$$(\text{EPS}) = \frac{1}{250\mu S + 25\mu S} = 3636 \tag{3.16}$$

3.7 Asynchronous Multiple-Access Constraints

The system described in this thesis utilizes the UWB radio to transmit tag ID's, replacing the 2.4 GHz transceiver. The mobile tags contain only a UWB transmitter. The lack of a tag receiver requires them to operate in an asynchronous transmit-only mode as proposed by [13]. They also points out that the major challenge of a transmit-only system is the high probability of collisions in a multi-user environment. Collisions occur because the tags operate asynchronously with no knowledge of each other or the transmission channel. In general, an asynchronous multiple access scheme should minimize the probability of collisions to maximize throughput, but also must eliminate the probability of clustered, called catastrophic, collisions. Clustered collisions are considered unacceptable because they can disrupt service temporarily even if their

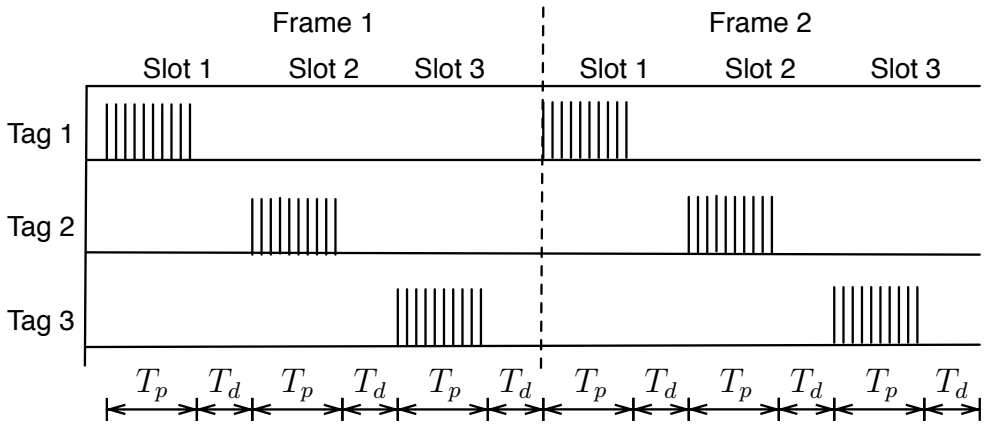

Figure 3.5: Diagram of a multi-tag localization system utilizing a synchronous multi-tag approach with packet duration T_p and switching delay T_d.

occurrence is rare. Ideally the occurrence of collisions should be uncorrelated in time, such that temporary service disruption due to repeated collisions is minimized.

Several collision avoidance schemes have been devised to address this problem, many utilizing some form of carrier sensing. One collision avoidance scheme proposed by [13] utilizes a different number of pulses per data bit to each user. By optimizing the number of pulses assigned to individual users they are able to improve bit error rate and system reliability. This scheme is not utilized in this work because of the difficulty in operating a sub-sampling receiver with transmitters utilizing different pulses per bit. Carrier sensing multiple access with collision avoidance (CSMA/CA) is another such scheme which was adopted as the MAC protocol for the IEEE 802.15.4 standard. In [14] orthogonal time hopping multiple access (OTHMA) was demonstrated to compare positively to CSMA/CA for low power, large scale, and low activity networks. For this work, we adopt the OTHMA scheme for multiple access because of its advantages for large scale and low activity networks, but also because it does not require a carrier detect capability which is challenging for UWB systems because of their low average power. Figure 3.6 shows the asynchronous system based on OTHMA that is used in this work. In this section, we adapt the probability of collision equations provided by [14] to our application, optimize the

multi-tag performance based on the probability of collisions, and finally discuss the potential limitations due to effects on localization accuracy

An equation for the probability of collisions for this system has been adopted from [14] as shown in (3.17).

$$P_c = 1 - (1 - \frac{\nu}{N_c})^{K-1} \tag{3.17}$$

The term ν is the user activity which is taken to be always one for this work since all tags are expected to transmit during every frame. The term N_c is the number of time hops in one frame which is taken to be the inverse of twice the packet duration (T_p) divided by the frame duration (T_f). It is twice the packet duration because a collision will occur if another tag begins transmission within one packet duration either before or after another tag transmission begins. Finally, the term K describes the number

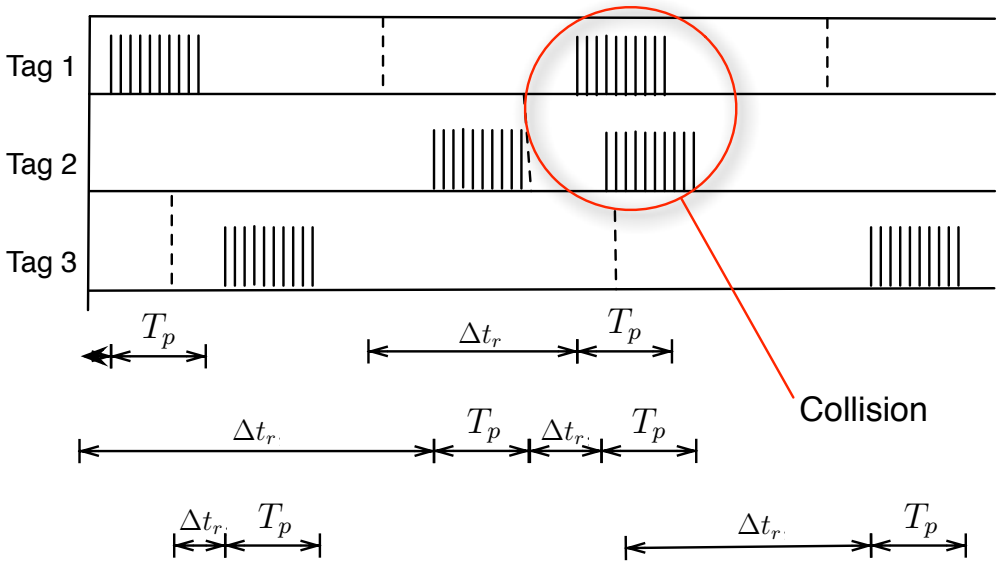

Figure 3.6: Diagram of a multi-tag localization system utilizing an asynchronous multi-tag approach based on OTHMA with packet duration T_p and a random time hop of Δt_r.

of tags. The adapted equation can be seen in (3.18).

$$P_c = 1 - (1 - \frac{2T_p}{T_f})^{K-1} \tag{3.18}$$

Figure 3.7 shows the relationship between number of tags and probability of collisions for 3 possible packet durations operating with 1 Hz refresh rate.

In OTHMA, time hopping is used to eliminate the possibility of catastrophic collisions by randomizing the offset of each transmission time. This reduces the probability of time correlated collisions between two tags. This work utilizes time hopping at the packet level to prevent catastrophic collisions while maintaining the time series information of the individual packet. The time when a packet transmission actually begins is randomized within the transmission frame using a pseudo random number generator. [14] This results in a uniformly randomized start time for each packet.

Packet collisions may result in a corruption of the packet that affects localization or tag-id transmission. In the worst case, we would assume that all collisions result in both packets being lost, but in fact typically some packets can be recovered even in the presence of collisions. Collision recovery is possible, because despite the overlap of two or more packets the probability of actual pulses overlapping is small due to the low duty rate of the UWB system. As seen in (3.19), packet collisions will reduce the effective refresh rate, R_{eff}, from the actual transmit rate, R, due to lost packets. This affects the multi-tag performance by reducing the ideal case by a factor of $P_c * (1 - P_r)$ as seen in (3.20).

$$R_{eff} = (1 - P_c * (1 - P_r)) * R \tag{3.19}$$

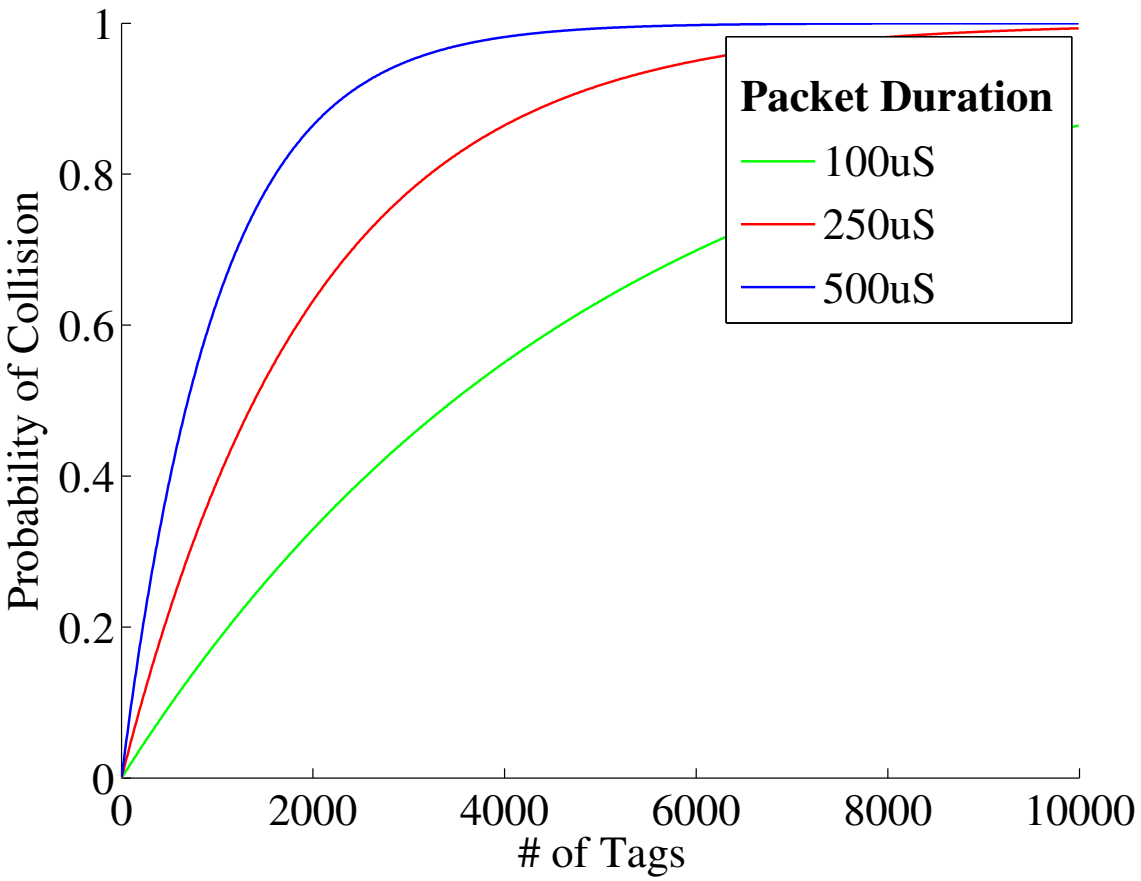

Figure 3.7: Probability of collisions by number of tags for three different packet durations all operating at a 1Hz transmit rate.

$$K * R_{eff} = \frac{1 - P_c * (1 - P_r)}{T_p} = \frac{1}{T_p} - \frac{P_c * (1 - P_r)}{T_p} \tag{3.20}$$

The probability of collision recovery, P_r, limits this effect, but even recovered packets may still have corrupted TDOA information reducing the accuracy of the system at high collision rates. The smoothing filter used in this work is also designed to be efficient at rejecting corrupted packets.

In order to simplify, we insert (3.18) for P_c in (3.19) and assume the number of tags, K, is two as used experimentally in this thesis. We then simplify to get an equation for events per second as seen in (3.21) to show the multi-tag performance

of the asynchronous system in the presence of collisions. For this thesis, the packet duration used is $149\mu S$ as seen in (3.8) and T_f is the inverse of the transmit rate, R. Figure 3.8 shows the multi-tag performance versus the tag transmit rate for both the worst case of no collision recovery and a case of 50% collision recovery.

$$(EPS) = 2R_{eff} = 2[R - 2T_p * R^2 * (1 - P_r)] \tag{3.21}$$

3.8 Conclusion

This chapter has introduced the performance metrics used to compare results in this paper, and developed a theoretical basis for the multi-tag performance of both the 2nd generation system and the proof-of-concept system developed in this thesis. The primary performance metrics used in this thesis are RMS accuracy for localization and a figure of merit for multi-tag performance, based on number of tags and refresh rate, called events per second. Theoretical performance was developed for an ideal TDMA system, a synchronous system similar to the 2nd generation system, and an asynchronous system similar to the one developed in this thesis. The next chapter further develops the proof-of-concept design and implementation of this system.

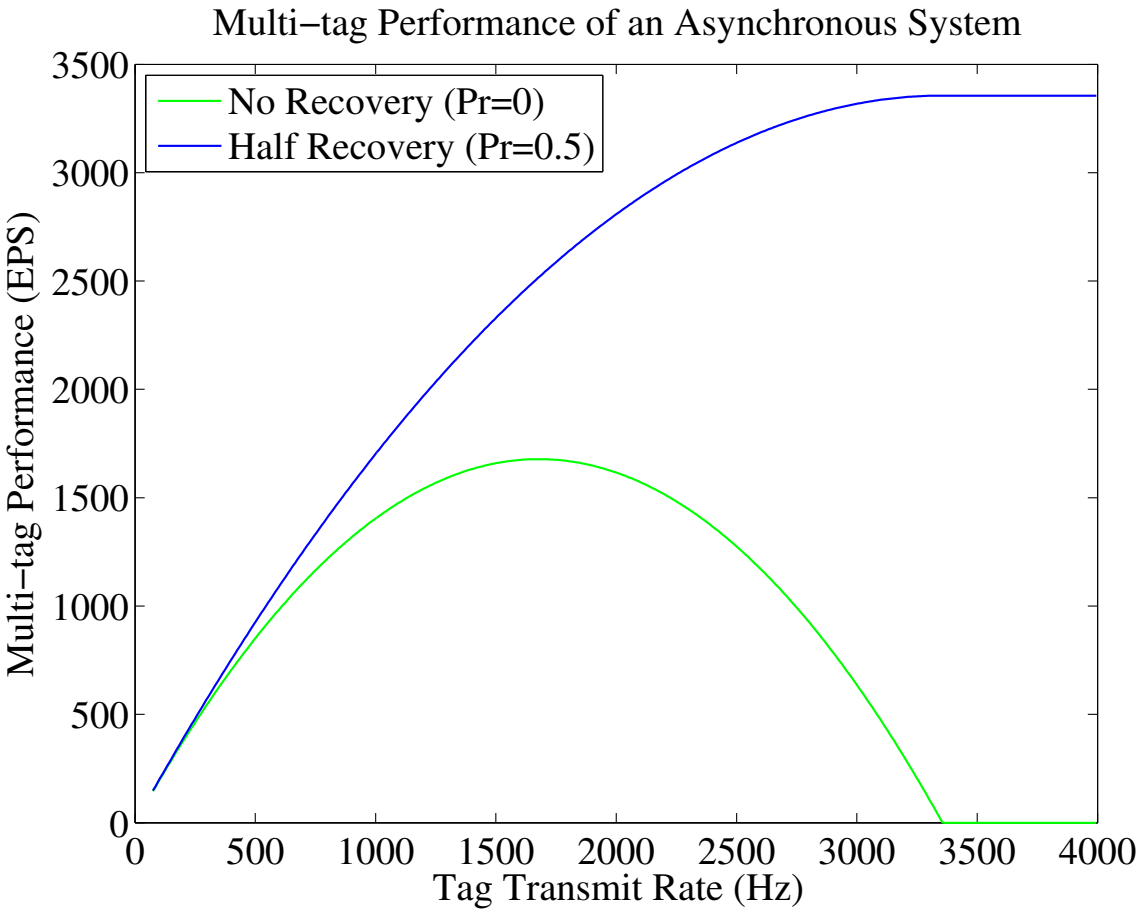

Figure 3.8: Multi-tag performance of an asynchronous system with 2 tags versus the transmit rate of the tags.

Chapter 4

Design and Implementation

4.1 Overview

An experimental system was designed and implemented that incorporates an orthogonal time hopping multiple access (OTHMA) scheme, digital communication using On-Off Keying (OOK) for tag identification, and high accuracy localization using sub-sampling based on prior UT work. The combined system design takes advantage of common hardware to accomplish these tasks, and limits the need for additional communications specific hardware. The implementation brings together a complete prototype system for experimental testing. This chapter begins by describing the communications scheme including multi-access, digital communication, and localization elements. The following sections describe the system implementation following the transmission path of the signals beginning with the tag and following through the base station, digital sampler, digital signal processing, and computer output.

4.2 Multi-Tag Scheme

The goal of this multi-tag scheme is the improvement of the multi-tag performance by reducing the localization time required for individual tags and eliminating the

need for a narrowband 2.4GHz transceiver by utilizing the UWB system for digital communications. This is accomplished without negatively impacting the localization accuracy of the system. The scheme allows for asynchronous transmit-only tags in order to keep down their cost, complexity, and power requirements. This section describes the developed multi-tag scheme, including the multiple-access method utilizing orthogonal time hopping multiple access (OTHMA), the operation of the localization scheme within the multi-tag framework, and the digital communications used to identify tags.

Each tags transmissions are organized into packets, each of which contains all the information necessary for a single localization and tag identification. The individual packets from multiple tags are organized into frames for the purpose of multiple access. The packet duration is determined by the requirements of localization. The duration of the frame is determined by the refresh period of the tags, which is the inverse of the refresh rate. The following sections describe the organization of the frames and packets.

4.2.1 Frame Organization

As stated above, a frame is a division of time equal to the refresh period of the tag. Each tag produces one and only one packet per frame. Figure 4.1 shows the relationship of frames from multiple tags and the organization of packets within them. Since the tags transmit asynchronously with no knowledge of each other, the frame boundaries of individual tags are randomly shifted in relation to each other. Also because of the asynchronous operation, there is some unavoidable probability of packet collisions. A packet collision occurs when two or more tags transmit packets that overlap in time. If tags were to transmit packets with a fixed timing within each frame then collisions between tags would be repeated during each and every frame. The result would be complete disruption of communication for the tags. This is referred to as a catastrophic collision. Catastrophic collisions are prevented by the

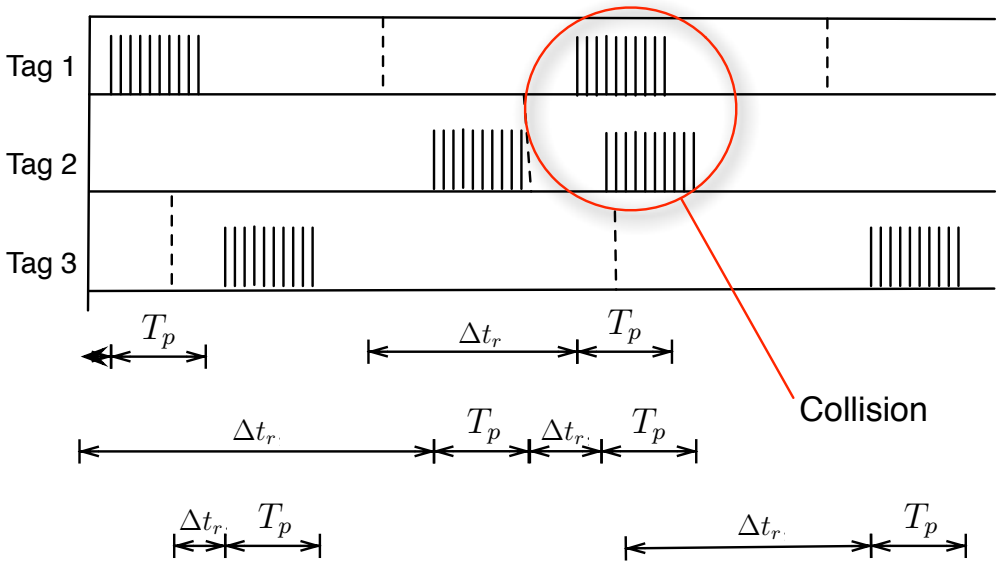

Figure 4.1: Organization of packets within transmission frames for three different tags. One collision is shown between packets transmitted by tags one and two.

application of time hopping which randomizes the location of the packet transmission within each frame. A pseudorandom number generator (pn-generator) is used to create orthogonal time hopping sequences for this purpose. Each pn-generator is seeded using the id of the tag copied out to fill the register, such that each tag has a unique sequence. Each packet is then transmitted at some effectively random delay, Δt_r, from the beginning of the tags frame boundary. The delay, Δt_r, is a uniform random distribution between 0 and the frame duration, T_f, minus the packet duration T_p. The packet is restricted from falling within one packet duration of the end of the frame to prevent the possibility of a tag interfering with itself during the following frame. Since the packet duration is small in comparison to the frame duration the effect on system analysis is negligible.

4.2.2 Packet Organization

Each packet consists of a preamble period used for localization followed by data transmission for the tag ID as shown in figure 4.2. Each packet is made up of a

series of UWB pulses produced at a constant rate of 10MHz. The preamble segment consists of unmodulated pulses which are used in the localization scheme. This is equivalent to transmitting a series of '1' data, or 'on' UWB pulses. The length of the preamble is dependent on the expansion factor used and the sampling period required to implement this. For this work the preamble is sized to exactly two times the required sampling period ensuring a high success rate in detecting transmitted packets. Ideally the preamble would be shortened to exactly the sampling period which is the minimum length for which the system can completely reconstruct the time period. The requirements for transitioning the system to shorter preamble lengths is discussed in chapter 6.

The base station subsamples the preamble to reconstruct the pulse shape. Figure 4.3 provides an example of subsampling. From the reconstructed pulse the base station identifies the peak position for use in the localization algorithm, and to determine the phase delay, or offset, between the base station sampling clock and received pulse. This phase delay is then used to synchronize the sampling circuit with the received pulses so that each of the following pulses in the packet can be sampled in real time. Typically, the packet will be detected and the sampling circuit switched to real time sampling well before the completion of the individual packets preamble. Movement of the tag is not a significant concern for the synchronization because the packet duration is so short, only $149\mu s$.

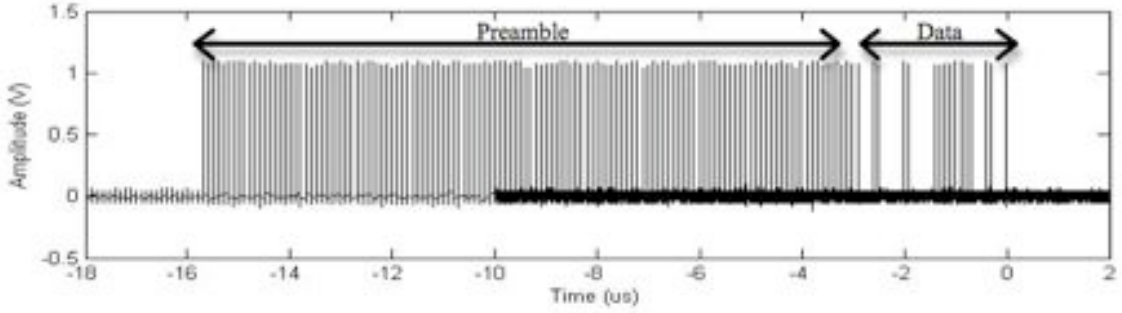

Figure 4.2: A full transmission sequence showing the preamble period used for localization and a data period used to transmit the tag identification.

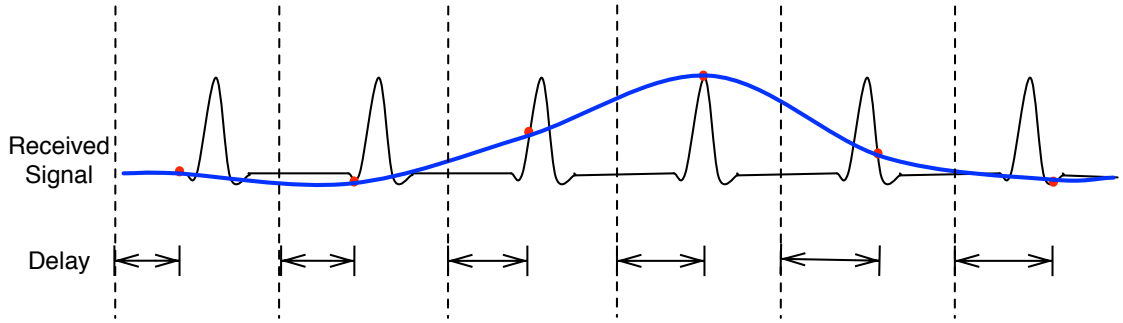

Figure 4.3: Example of sub-sampling done on the preamble of each packet. The delay is slowly increased across the sampling period. The black curve is the received signal and the blue curve is the time extended reconstruction.

The preamble is followed immediately by the data transmission using on-off keying (OOK) modulation of the UWB pulses as seen in figure 4.4. The data transmission begins with two '0' start bits to identify the end of the preamble and beginning of data transmission. This ensures data reception is aligned with the tag ID transmission. The base station is able to sample each period of the data, because the sample clock has been synchronized with the received pulse during the preamble. Each sample during this period is compared with a threshold value for conversion to digital data. In our implementation, the start bits are followed by the 16 bit tag id. This completes the transmission sequence.

4.3 Tag Hardware

The tags consist of three primary parts: a digital controller, a UWB transmitter, and an antenna. The digital controller sets the update rate for the tag, implements time hopping, sets the length of the preamble, and stores the 16 bit identifier unique to each tag. The UWB transmitter takes a digital input signal and converts it to a UWB output signal that is transmitted over the air via the omnidirectional antenna. Figure 4.5 shows a simple block diagram of the tag. The system is made up of multiple tags. Two of which were implemented for this experimental system.

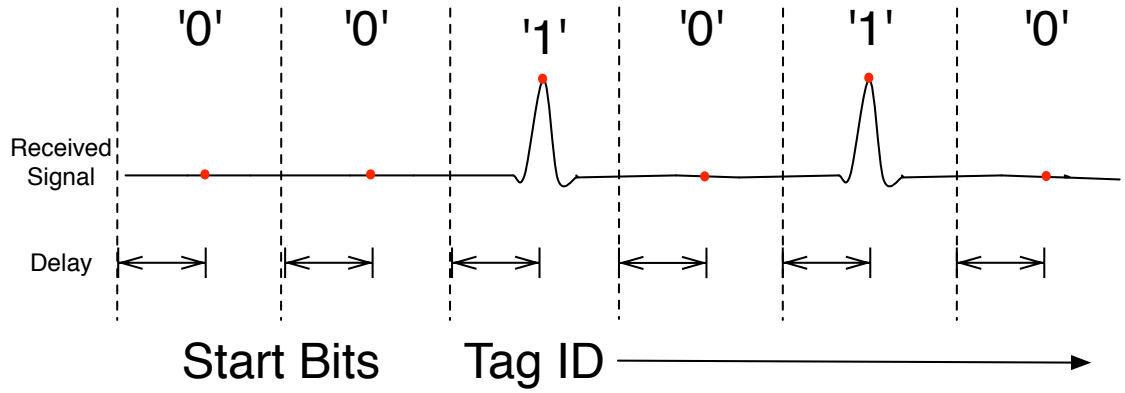

Figure 4.4: Example of real-time sampling used to recover the tag-id during data transmission. During real-time sampling the delay is held constant.

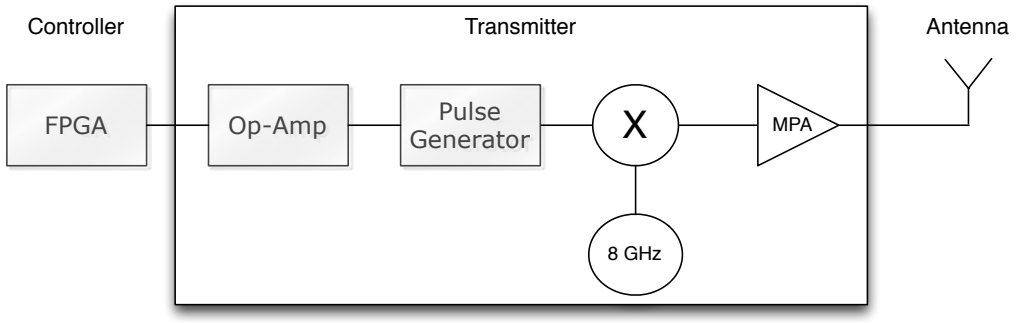

Figure 4.5: Tag schematic showing the controller, transmitter, and antenna.

4.3.1 Controller

The controller is a digital microprocessor or FPGA capable of generating the tag output required by the multi-tag scheme. For the prototype system, a Xilinx SP605 development board with a Spartan 6 FPGA has been used for digital control. The FPGA was selected because of its excellent performance at the required 10MHz transmission rate and because of it flexibility in prototyping. Ideally, future tag designs will move to a low cost and low power micro controller platform. An SMA output from the development board drives the UWB transmitter. The FPGA development board is powered through an included DC supply, and has an onboard

100MHz oscillator that is down sampled to 10MHz. The FPGA is programmed in VHDL to implement the multi-tag scheme.

The VHDL code consists of a transmission state machine as shown in Figure 4.6, a Xilinx provided "coregen" clocking wizard to generate the internal 10MHz clock, and a PN-generator for producing pseudorandom numbers used as the orthogonal time hopping sequence. [15] The state machine generates a data output for the tag that is combined via an 'AND' with the 10MHz clock to create the output that drives the UWB transmitter. This is required because the UWB transmitter is driven by a rising edge. Figure 4.7 shows the input to the transmitter required for generating digital data.

The transmission state machine is synchronized on the 10MHz clock. It consists of 4 states that together make up one frame for the tag. States 1 and 4 are delays that together implement the time hopping. States 2 and 3 implement the packet transmission with 2 producing the preamble and 3 producing the tag ID.

The time hop for each frame is calculated at the end of the proceeding frame. It is based on a pseudorandom number taken from the current state of a PN-generator described in the following section. This pseudorandom number R_n, between 0 and the frame duration, T_f, minus the packet duration, T_p, is used as the delay for state 1. The delay for state 4 is the pseudorandom number R_n subtracted from the frame duration, T_f, minus the packet duration, T_p. The entire frame then has a constant duration as shown in (4.1). The data output is held low throughout the delays of states 1 and 4.

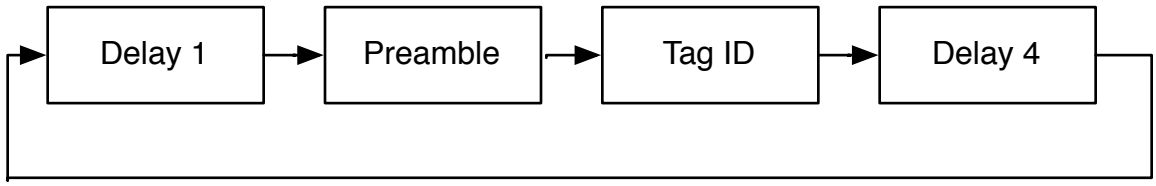

Figure 4.6: State machine used by the digital controller to generate the required transmission sequence.

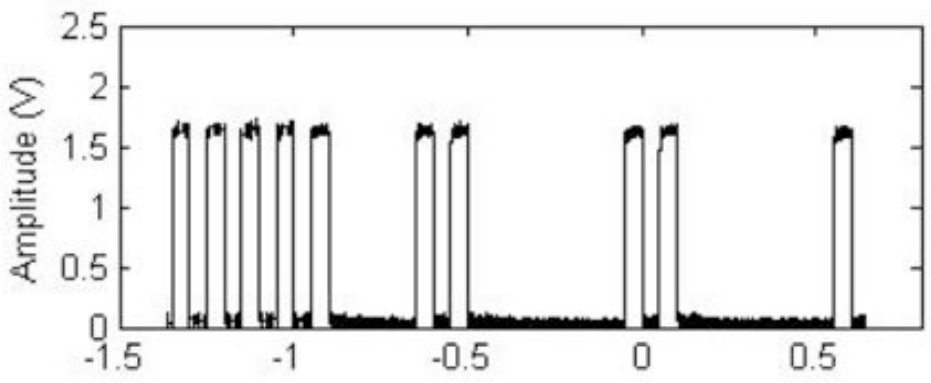

Figure 4.7: Data source from the digital controller that drives the UWB transmitter showing the end of the preamble and beginning of the tag id transmission.

$$Delay_1 + T_p + Delay_2 = R_n + T_p + (T_f - T_p - R_n) = T_f \tag{4.1}$$

The packet transmission consists of a preamble and a tag ID transmission. State 2 generates '1' or 'on' UWB pulses for the duration of the preamble. State 3 generates the 16 bit tag ID using a shift register that is preloaded with the ID. As a convention tag ID's are transmitted beginning with the most significant bit and ending with the least significant bit, or Big Endian, so for example tag 5A80 would begin "0101" and end with "0000".

4.3.2 Psuedorandom Number (PN) Generator

A maximum length linear feedback shift register (LFSR) is used to generate the random time hops for each tag. A 63-bit LFSR configuration with feedback taps at 63 and 62 was selected for this purpose from a Xilinx Application Note.[16] This configuration has a repetition time of $(2^{63} - 1)$ clock periods. At our 10 MHz clock rate, this PN-generator will repeat every 29,247 years, which can effectively be ignored for practical purposes.

Only the last 17 bits of this shift register are utilized in setting the delay for time hopping. Because of the overall length of the register and the long repetition period the time hop delay can effectively be considered uniformly random for analysis purposes. A possible problem with using LFSR is that if two registers ever align due to starting points or clock drift, they will remain aligned since the sequence in every LFSR is identical. To reduce this possibility each shift register is seeded with the tag id duplicated out to 63 bits. This coupled with the length of the register makes it unlikely that any two will ever align.

4.3.3 Transmitter

The transmitter, shown in Figure 4.8, consists of an op-amp based comparator, pulse generator, mixer, local oscillator, and medium power amplifier. The pulse generator and up conversion are the same as used in past transmitter designs. [6] The pulse generator is triggered by a rising edge in the data and produces a 300ps pulse which is up-converted to 8GHz for transmission. In past transmitter designs the pulse generator has been triggered directly by a 10MHz clock source with no method for sending data.

The data source provided by the controller serves to provide a trigger for the generation of pulses. An op-amp comparator circuit is used to convert the 0 to 3V logic level signal from the controller to a -5V to +5V signal required by the pulse

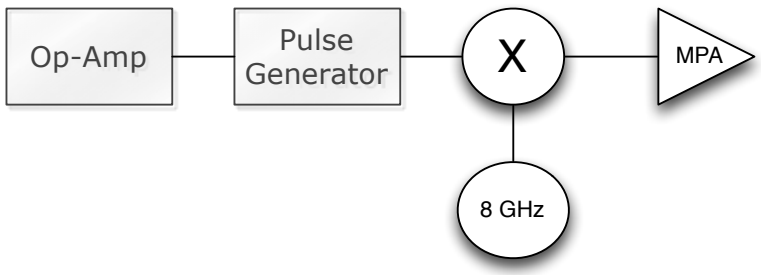

Figure 4.8: Schematic of the UWB transmitter.

generator, and to supply the high instantaneous current required. The pulse generator is triggered by the rising of edge of this signal and generates a 300ps pulse, as measured at the full width half max. The pulse generator is based on a step-recovery diode circuit from [12].

The 300ps pulses have a bandwidth of around 3 GHz centered at baseband. These pulses are then up-converted to 8GHz using a hittite HMC553 mixer for transmission. The selected mixer has excellent LO to RF isolation, which is required in this application to prevent continuous LO leakage from dominating the low duty cycle transmission. A free running VCO centered at 8 GHz is used as the LO. This simple low-cost LO can be utilized since frequency drift of the LO is accepted by the non-coherent receivers. An HMC441 medium power amplifier is used at the output to boost the signal for transmission. The transmitted signal approximates the FCC 3.1-10.6 GHz mask though the power level typically exceeds the limits due to carrier leakage at 8 GHz. The average power spectrum of the transmitted signal can be seen in figure 4.9. An omni-directional antenna is used for the tag transmission since the orientation of the tag to the base-stations is unknown. The antenna can be seen in figure 4.10.

4.4 Base Station

Each base station has an antenna and RF front-end consisting of an input filter, RF receiver, and baseband amplifier as seen in Figure 4.11. The base station receives the UWB signal, down converts it to baseband, and amplifies the signal. The output of each base station is connected back to a central digital sampling circuit for processing of the baseband signals. In this work, two base stations were used for 1-D ranging. In a 3-D localization system, a minimum of four base stations would be required and additional base stations could be utilized for improved range, accuracy, or reliability.

The base station antenna is a directional Vivaldi antenna, seen in figure 4.12, that provides moderate directionality and associated gain. The approximate phase

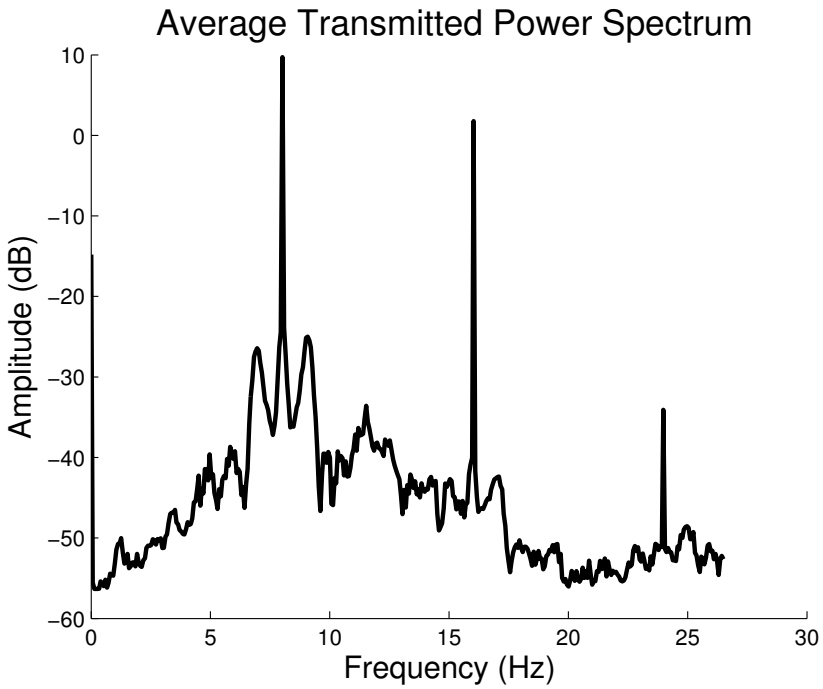

Figure 4.9: Average transmitted power spectrum for the upconverted UWB signal.

center of each base station antenna is measured as this represents the receive point for time of flight measurements from each tag. The antennas for each base station are positioned at the desired receive point and aimed for optimal performance in the region of interest. The antenna is connected to the RF front-end using a high frequency rated SMA cable.

The RF front-end begins with a passive 5-11GHz filter to limit the noise and interference at the receiver. The filter is followed immediately by the RF receiver which is an integrated SiGe MMIC circuit provided by the Institute of Electronic Devices and Circuits at the University of Ulm. [17] The receiver utilizes a non-coherent, energy detection method for down-conversion. The non-coherent receiver is advantageous as it operates well even in the presence of frequency drift in the local oscillator on the tags. After the receiver, either one or two baseband amplifiers are used depending on range to adjust the signal level for optimum performance of the digital sampler.

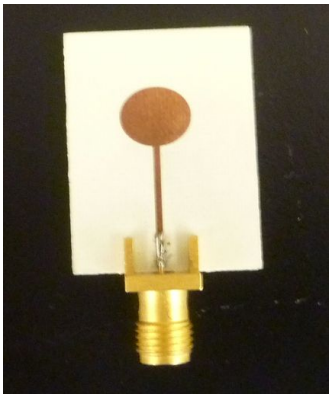

Figure 4.10: Omni-directional antenna used with the tags.

4.5 Digital Sampler

The base station utilizes the digital sampling circuit shown in 4.13. It consists of a Virtex 5 FPGA, a digital programmable delay chip, a 150MHz clock source, and a fast high bandwidth ADC. It is the part of the base station used to sample incoming signals, identify the pulse position for localization, and to receive digital data for tag identification. The sampling circuit is used in two modes: sub-sampling and real-time sampling and follows the flow diagram in figure 4.14.

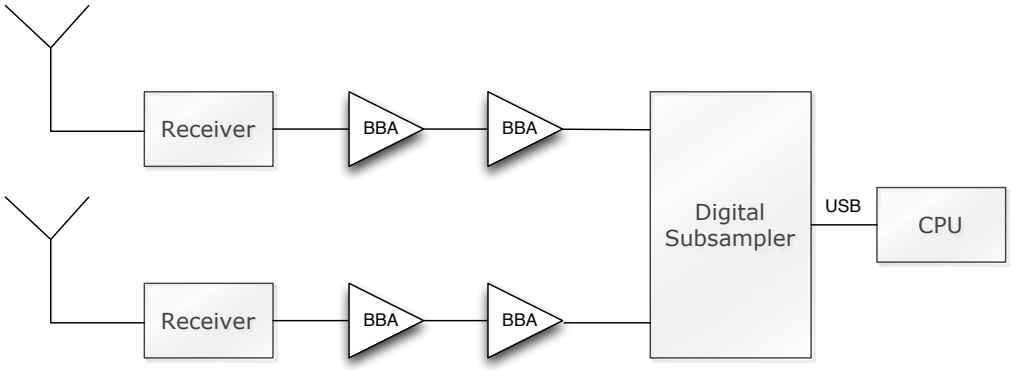

Figure 4.11: Diagram of two base stations connected to a dual input digital sampler that interfaces with a data collection PC.

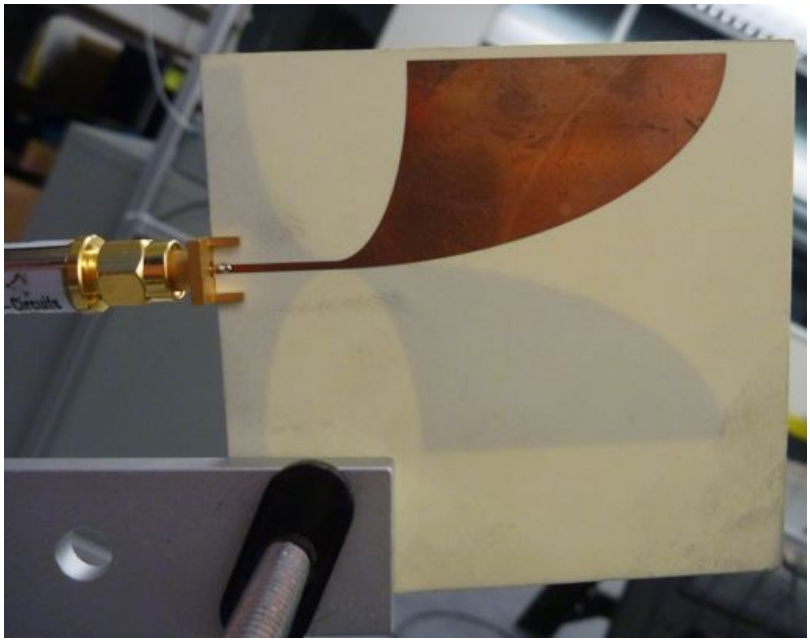

Figure 4.12: Directional Vivaldi antenna used with the base stations.

The sampling circuit begins in sub-sampling mode. Sub-sampling is implemented by incrementally adjusting the phase of a 150MHz clock using the digital programmable delay chip. This shifts the position of samples across a periodic signal, and allows reconstruction of the signal shape at much greater resolution than could be achieved at the available sampling speed. A sample resolution of less than 10ps can be achieved based on the minimum programmable delay. The sampling clock of 150MHz is 15 times faster than the transmit clock. This allows 15 samples to be recovered per transmission period. Every second transmission period is skipped in order to allow for adjustment of the delay chip. This allows us to reconstruct the pulse shape 7.5 times faster than the analog sub-sampling method used in the previous UT system. This allows us to reconstruct a single period, with an expansion factor equivalent to 11,160, in 148.8 μS with only 1,488 pulses. After a full period has been sampled, the peak sample value is compared with a fixed threshold to separate received pulses from the noise. For this work, a threshold of $\pm$76.3 mV, equivalent to 2500 in the ADC, was selected based on typical noise values and peak heights observed during testing. If the peak value exceeds the threshold then a pulse has been received and real-time

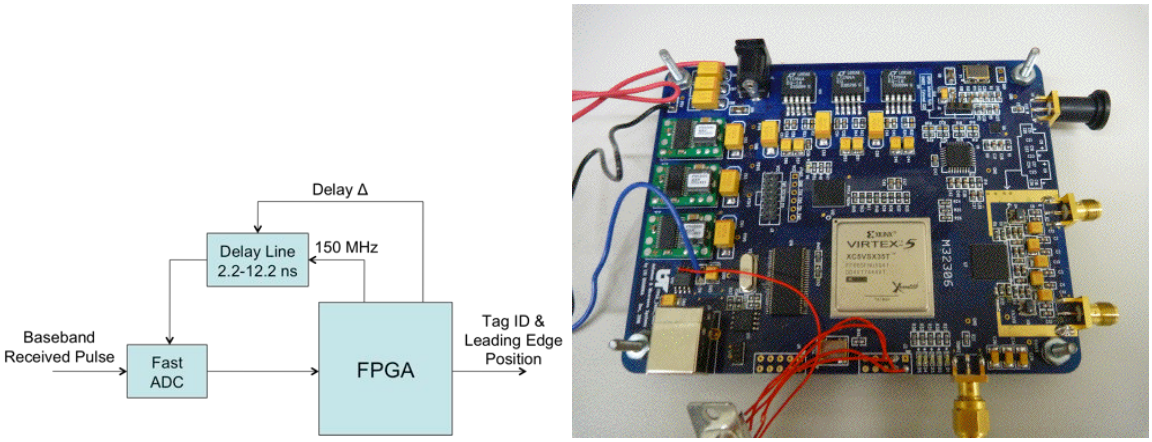

Figure 4.13: Schematic (a) and picture (b) of the digital sampler circuit.

sampling begins, otherwise no pulse was identified and sub-sampling continues for another period.

In the real-time sampling mode, a fixed delay is set that synchronizes the phase of the sample clock with the center of the received pulse train. The fixed delay is based on the delay of the peak sample identified during sub-sampling. By setting correct delay adjustment, every period of the transmitted signal can be sampled allowing reception of digital data. Some clock drift may occur between the time that the pulse is identified in subsampling and the time that the data is read during real-time sampling. After testing, a fixed offset has been used to account for the average clock drift between the transmitting tags and the receiver. A fixed offset of -450 pS, or 45 samples, has been used for this work. After the fixed delay is set, a sample is taken each clock period and compared to a threshold. Samples above the threshold are assigned as 1's, and those below are assigned as 0's. The start of the tag-id is identified by two 0 bits. If 2,750 clock periods pass without the start of a tag-id then an error is reported and sub-sampling begins again. After the reception of two 0 bits, the following 16 samples are stored as the tag-id in a 16-bit shift register. A maximum data rate of 10MBits per second can be achieved using this method.

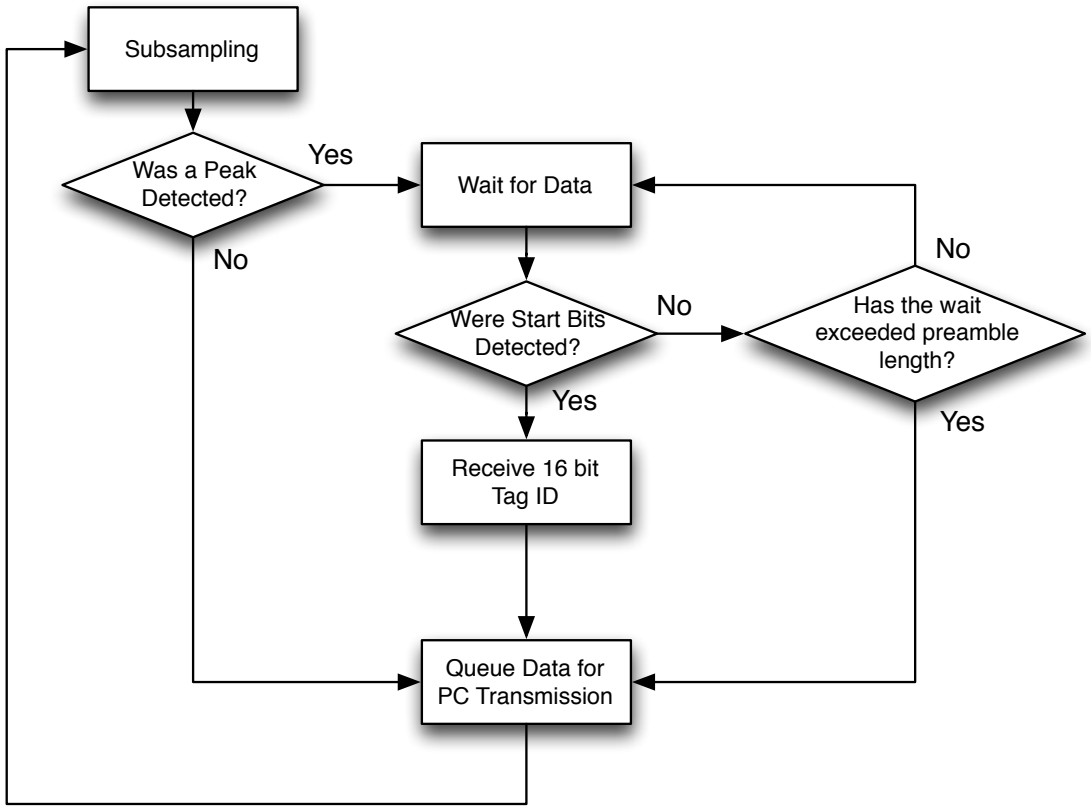

Figure 4.14: Diagram of the FPGA state machine used in the digital sampler.

The resulting peak amplitudes and peak sample times from both base stations are reported along with the tag-id over a USB connection to the computer. The USB is operated asynchronously to the sampling using a first-in first-out (fifo) register. The USB communication with the computer operates at 48 MHz and can occur simultaneously to sampling. The fifo register is cleared upon connection of the interface software, and overflows of the register are monitored and trigger an overflow indication LED on the sampling circuit.

4.6 Computer Interface

The computer interface with the digital board is a C++ software application developed in Microsoft Visual Studio. It allows data collection from the digital

sampling board over a user selectable time period. Data is received from the USB connection and stored in a user designated file in the format shown in Table 4.1. This data is then analyzed in Matlab to generate positional results and separate results by tag-id.

Table 4.1: File format for data collected through the PC interface software.

Byte #	Description	Example
1	Peak value from A channel	32768
2	Peak value from B channel	32768
3	Time index of peak from A channel	10066
4	Time index of peak from B channel	10143
5	Leading edge index from A channel	11
6	Leading edge index from B channel	8
7-9	FPGA Timestamp (in 6.667 ns increments)	4236158
10	Tag ID	12483
	(Repeat)	

4.7 Conclusion

This chapter has described the experimental system that was developed based on the OTHMA scheme used for multi-tag access, OOK for digital communication of tag id's, and TDOA for localization. The system utilizes the same UWB transmitter and receiver used in past work on the UT localization system. A digital sampling board originally designed for a UWB see-through-walls system was adapted for use in localization. The digital sampler allows for both sub-sampling used in localization and time synchronized real-time sampling for tag-id reception. A computer interface allows data from the digital sampler to be recorded and then analyzed in Matlab. This system implementation is used in the experiments in the following chapter to demonstrate the system performance.

Chapter 5

Experiment

5.1 Setup and Data Collection

The experimental setup consists of two base station antennas fixed at opposite ends of a track containing two movable tag antennas. An Optotrak 3020 system is positioned to view the entire setup. The Optotrack system has localization accuracy of .3mm and is used as a ground truth reference for the experimental results. [18] The base station, tag electronics, and digital sampling board are positioned along and under the track. The experimental setup can be seen in figure 5.1.

All optical positions were measured manually using a handheld probe. The position of the base station antennas was measured to the expected phase center as indicated in figure 5.2a. The tag antennas were measured to a point near the phase center as indicated in figure 5.2b. Positions are measured over 200 updates of the optical system and a standard deviation of less than 1mm was required for all optical measurements.

Two experiments were conducted with this system to measure different system parameters. In both experiments, two tags were utilized simultaneously to analyze multi-tag performance. They are identified by the arbitrarily assigned tag-id's of 45655 and 12483. The first experiment measured the multi-tag performance over a

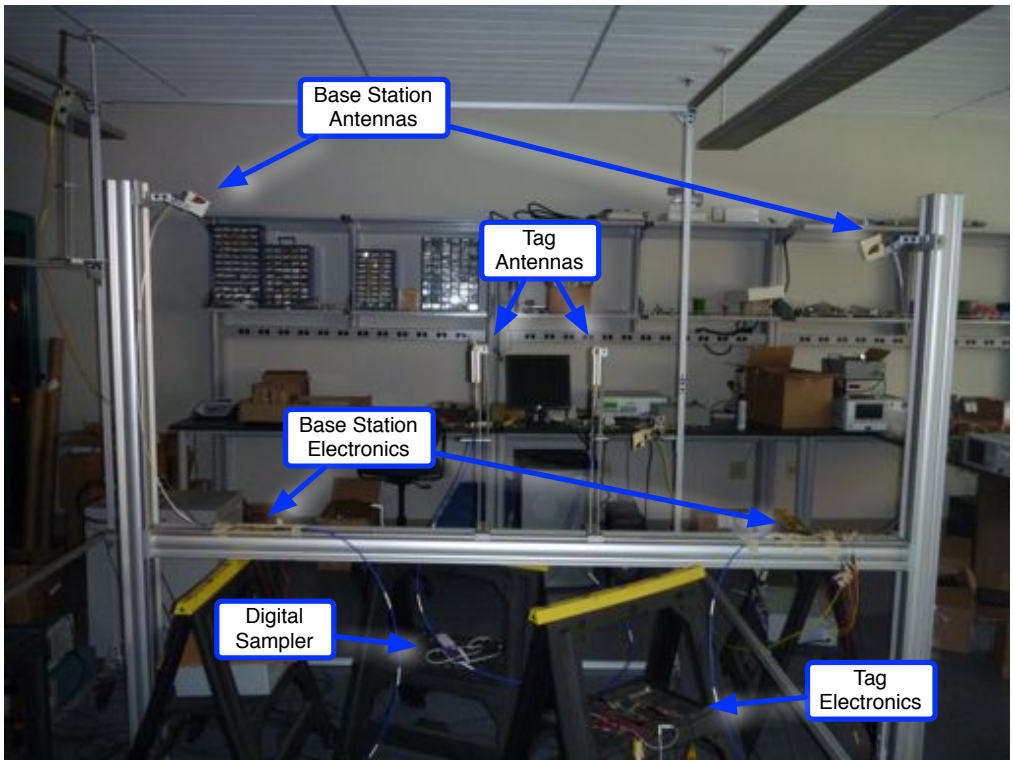

Figure 5.1: Experimental setup including two base stations and two tags.

range of tag transmit rates. The localization accuracy at each of the tag transmit rates was also compared based on the standard deviation of the static tags TDOA. Based on this experiment a tag update rate was selected that would balance a good multi-tag performance with high localization accuracy. The second experiment was conducted with a fixed update rate and a tag moving through 10 different points. The first 5 points are used as a calibration to fit a linear relationship between TDOA and position, and the position accuracy of the remaining 5 points based on this linear fit is used as the measure of localization accuracy. A similar experiment was conducted with the 2nd generation system to provide a fair comparison of results.

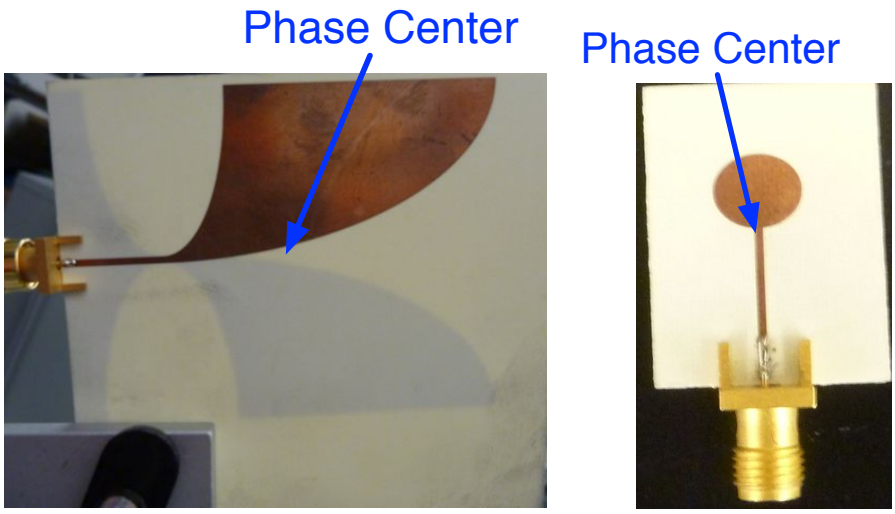

(a) **(b)**

Figure 5.2: The phase center location of the base station antenna (a) and the tag antenna (b).

5.2 Update Rate Experiment

The first experiment was designed to measure the relationship of accuracy and multi-tag performance to tag transmission rate. For this experiment, 9 different tag transmission rates were used ranging from 75Hz up to 3306Hz. At each transmission rate, data was collected for approximately 60 seconds with both tags active. Accurate data collection time is measured based on timestamps originating with the data in the FPGA and resulted in 61.6 seconds for each period. The positions of the tags were kept fixed throughout the experiment. The standard deviation of the TDOA measurements are used as a rough measure of accuracy since calibration curves were not generated for each transmission rate. The standard deviation is directly proportional to the random measurement error, but discounts calibration error.

The data for each of the measurements was processed using Matlab. The data for each transmission rate was stored in an individual file in the form described in section 4.6. During processing, the data was separated based on tagID and the TDOA was calculated, in number of samples, by subtracting the index of the channel two

peak from the index of the channel one peak. The resulting TDOA measurements are filtered to remove outliers and reduce higher frequency variation. A detailed description and analysis of the filter used in this work is provided in the following section 5.3. The mean and standard deviation of the filtered TDOA was calculated for each position along with the update rate in tags per second averaged over the entire measurement period. A summary of the results is provided in table 5.1.

Table 5.1: Update rate experiment data summary.

		Tag 12483		Tag 45655	
Frame Delay	Transmit Rate	Update Rate (Hz)	Accuracy (mm)	Update Rate (Hz)	Accuracy (mm)
255	3306	1281.9	28.62	1337.4	17.46
511	3048	1111.9	25.52	1311.2	7.00
1023	2636	1247.3	16.00	1017.6	10.77
2047	2076	1081.6	10.86	1250.8	22.62
4095	1457	1056.3	6.99	1028.7	22.64
8191	912	704.1	5.99	731.4	27.99
16383	522	431.3	5.21	447.6	29.64
32767	281	238.5	4.37	255.6	29.31
131071	75	69.1	4.71	69.1	31.56

The experiment shows that as expected both system update rate and localization accuracy are directly affected by tag transmission rate. The system update rate increases with tag transmission rate as seen in figure 5.3, but because of collisions approaches asymptotically some maximum update rate around 1200Hz to 1300Hz. At high tag transmission rates the affect of collisions results in degraded performance of the multi-tag system. The localization accuracy also appears to be affected by the tag transmission rate. Figure 5.4 shows the increase in standard deviation of the TDOA measurements as tag transmission rate increases. This would directly result in a decrease in localization accuracy. Localization accuracy was only compared for tag 12483 which was near the center between the two basestations. Tag 45655 was outside the primary experimental region resulting in high uncertainty in the localization

measurements. From this data a tag transmission rate of 912Hz was selected for use in the accuracy experiment because it balances the desire for localization accuracy and high update rate.

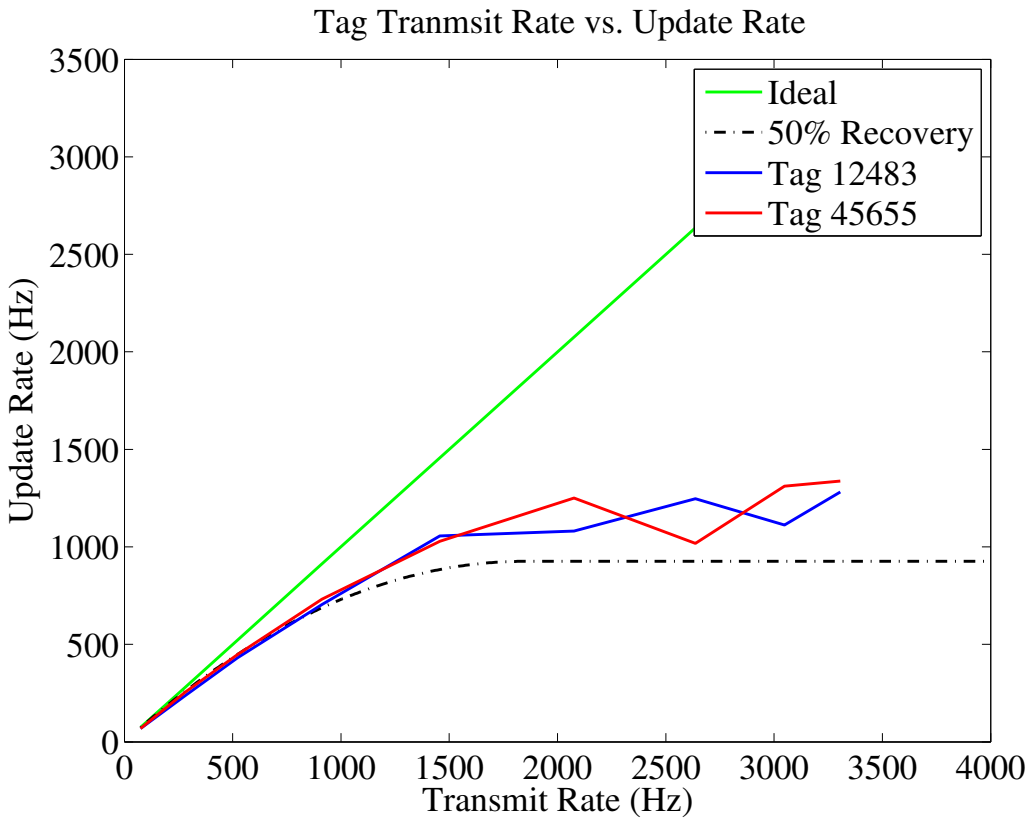

Figure 5.3: Plot comparing the effect of collisions on update rate in the real system to the ideal update rate with no collisions.

5.3 Data Filtering

Filtering of the TDOA measurements is done by mean filtering with outlier rejection to reduce variance and limit the effect of non-gaussian outliers. Filtering is done on a window of samples sliding across the entire data set. The size of the window is adjustable and analysis was performed for filters with 80 and 160 sample window sizes. For each sample window, 50% of the data points with the greatest euclidean

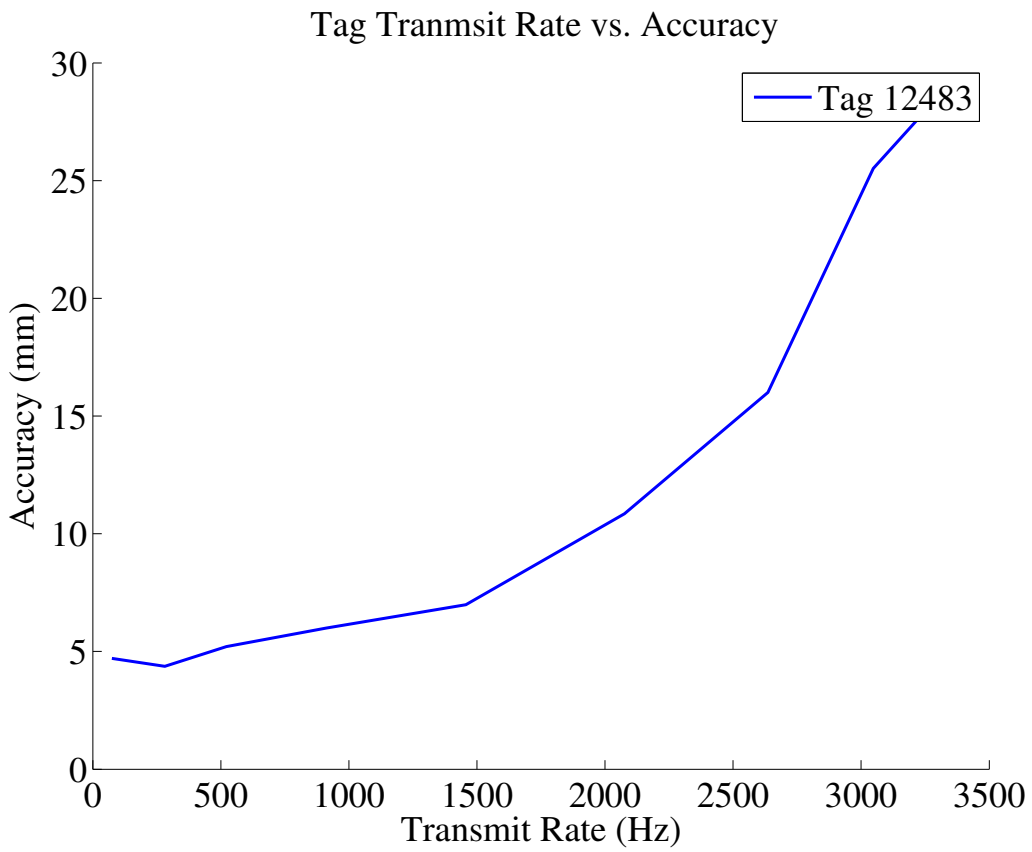

Figure 5.4: Plot showing the effect of collisions on the localization accuracy at high transmit rates.

distance from the sample window mean are eliminated from the set. The remaining samples are averaged to get the filtered value.

This filter was selected over a standard mean filter because of the existence of a significant number of non-gaussian outliers. These outliers may be the result of interference or noise affecting one or both base stations, or the effect of collisions in corrupting TDOA measurements. Figure 5.5 compares the unfiltered TDOA measurements with the result of a simple mean filter and the mean filter with outlier rejection for a single point of the 912Hz transmit rate experiment. In Figure 5.5b, it can be seen that the mean filter is heavily affected by a group of outliers near zero. The filter with outlier rejection, in figure 5.5c, is centered closer to the main peak of the unfiltered data, because it limits the effect of these outliers. The reduction in

outlier effect also reduces the spread in data for this filter over the simple mean filter. The effect of each filter on the histogram peak, mean, and standard deviation for the example data can be seen in Table 5.2.

Table 5.2: Comparison of filtering methods on histogram peak, mean, and standard deviation. A bin size of 10 samples was used for determining the histogram peak.

	Peak	Mean	Std Dev
Unfiltered	0.00	17.30	450.64
Mean Filtered	-3.00	17.38	35.16
Mean Filtered with Outlier Rejection	11.00	10.62	1.22

5.4 Accuracy Experiment

The second experiment was designed to measure the system update rate and localization accuracy with a fixed tag transmission rate and realistic calibration scenario. The experiment is conducted with both tags active to demonstrate multi-tag effects, but only tag 12483 is used for accuracy measurements. Data is collected for approximately 60 seconds at each of 10 different locations spanning a 200mm length. The first 5 points are used to generate a calibration for the system relating average TDOA measurement to linear position as measured by the optical system. The linear position of the remaining 5 points is then calculated based on this calibration, and compared to the position as measured by the optical system. For each position, the localization accuracy, as compared to the optical system, and the multi-tag performance, based on system update rates, is reported.

The system calibration is set by fitting a curve between the linear position of the tag as measured by the optical system and the average TDOA as measured by the UWB system. For this experiment 5 points at positions across the length of the experiment were used for calibration. A linear fit of the form $y = ax + b$ was used because of its physical relationship to the measurement system. For a linear fit, the

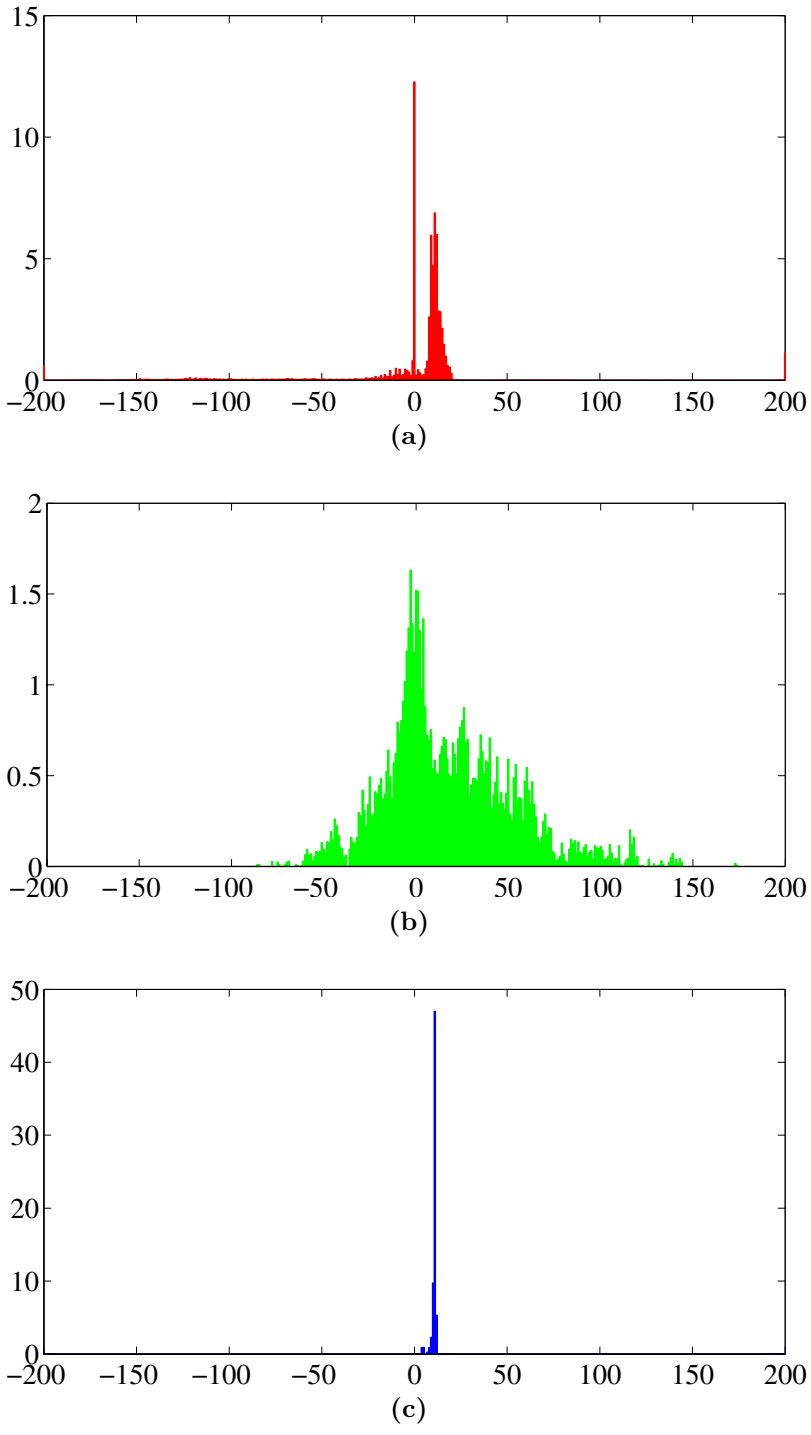

Figure 5.5: Comparison of (a) unfiltered TDOA measurements with the results of measurements filtered by (b) a simple mean filter and (c) a mean filter with outlier rejection.

Table 5.3: Accuracy experiment data summary for tag 12483 with 160 sample filter window.

Location	System Update Rate (Hz)	Optical TDOA (ps)	Average Position (mm)	Calculated Position (mm)	RMSE (mm)
1	861.7	-82.18	-99.74		
2	878.2	-52.37	-50.68		
3	882.9	-19.75	0.00		
4	897.2	10.62	49.86		
5	886.3	45.37	100.12		
6	896.8	-53.24	-50.39	-53.13	2.60
7	896.3	-32.78	-19.33	-20.97	2.54
8	901.4	-19.89	0.08	-0.71	1.43
9	896.7	-2.98	20.98	25.88	5.83
10	893.5	10.50	50.22	47.06	3.82
Avg:	889.1			Avg:	3.25

a coefficient takes into account the scaling associated with the expansion factor from subsampling, and the b coefficient takes into account fixed delay differences associated with cable length or receiver component differences. The linear positions are all reported with a 0 reference at the midpoint between base stations. The coefficient of determination, R^2, for this linear fit is 0.9998 which indicates that the linear fit is an excellent model for the calibration. The calibration data and resulting curve can be seen in figure 5.6. The resulting a and b coefficients are 1.57 and 1115 respectively.

5.5 Conclusion

The results of the two experiments show successful multi-tag operation for two tags. The update rate experiment demonstrates a trade-off between tag transmission rate and localization accuracy, and also shows the effect of collisions in reducing system update rates when tag transmission rates become high. The accuracy experiment

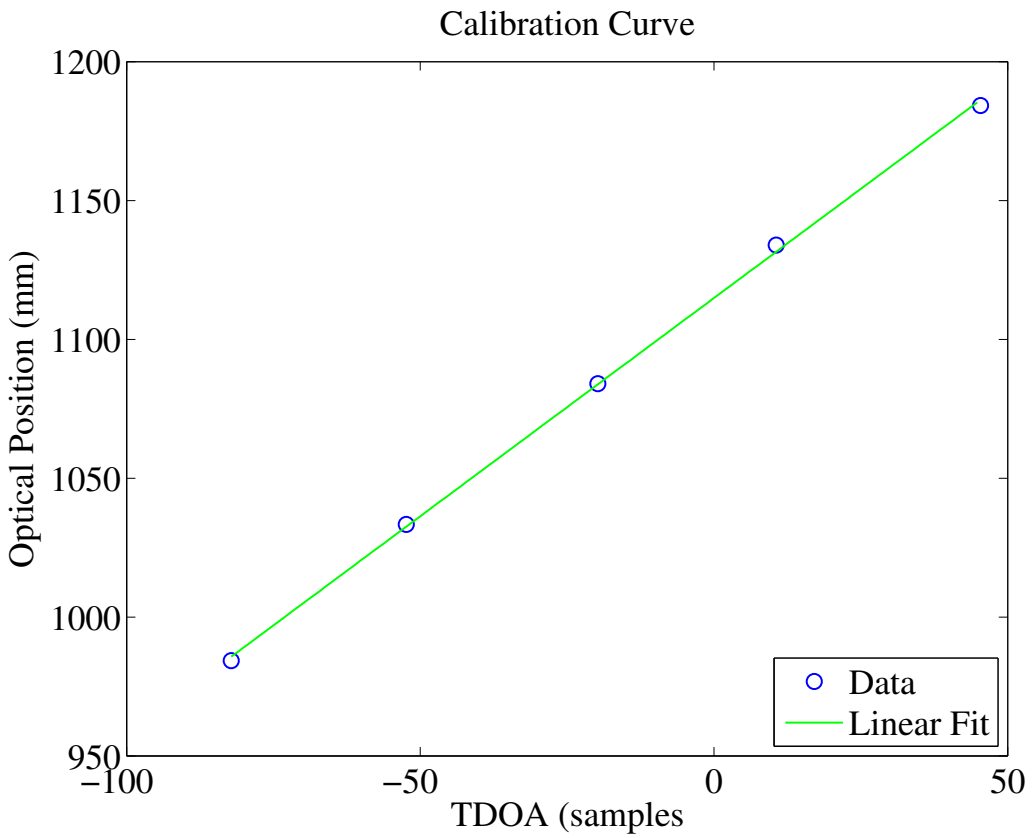

Figure 5.6: Linear calibration curve relating the TDOA measurements in samples to the optical ground truth data in millimeters.

demonstrates successful calibration of the system allowing calculation of linear 1-D positions using the UWB TDOA measurements. The calibration and accuracy measurements were demonstrated in the presence of multi-tag interference.

It is difficult to compare these results with past reported results for the UT system, because of differences in the experimental parameters such as 1-D localization instead of 3-D and static positions instead of dynamic tracking. In order to provide a fair comparison with the 2nd generation system, the accuracy experiment as conducted in this work was repeated for that system. As far as possible the same positions and data collection times were used. The resulting comparison is provided in Table 5.4.

Table 5.4: Summary of experimental results comparing this work with results from the second generation system.

	2nd Generation		This Work	
Filter Window	Accuracy RMSE (mm)	Update Rate (Hz)	Accuracy RMSE (mm)	Update Rate (Hz)
80	3.86	583.9	4.75	889.1
160	3.72	587.7	3.25	889.1

Chapter 6

Next Steps

The system developed through this work represents only an initial proof-of-concept design. A number of areas for potential improvement have already been identified, and the work to-date has identified several areas where future research may be conducted to further improve system performance. The "Next Steps" provided here are not necessarily a plan for system development, but rather concepts coming from this work for consideration in future efforts.

6.1 3-D Dynamic Tracking

The system implemented as a part of this thesis work only provided for 1-D static localization of tags for a proof-of-concept. Expansion to dynamic 3-D tracking of tags should be possible based on the existing architecture with the addition of 2 or more base stations and the associated necessary sampling hardware. Additional antennas and receiver circuits for use in base stations already exist. The limitation is the digital sampling circuit which currently has only 2 channels. There are two possible options for expanding the number of base stations: multiple 2-channel digital sampling circuits could be synchronized using a common clock source, or a new digital sampling circuit could be fabricated to include 4 plus channels. The digital signal processing on the computer would have to be modified to allow for a 3-d calibration

and 3-d point calculation. The methods and algorithms for this already exist in the 2nd generation system and could be adapted to the new system.

6.2 Optimized Preamble Duration

As mentioned in chapter 4, the optimal preamble duration is equivalent to the sampling period. In this work the preamble has been sized to twice the sampling period to ensure a high rate of success in identifying the packet and receiving the tag id. This requirement is due to the discrete, one period at a time, method of sub-sampling the pulse such that one sampling period is collected, analyzed, and then the process repeats. If the preamble is only one sampling duration, it is possible and relatively likely that a tag may begin transmitting during one sampling period such that it is missed during this period and then transmission will end before the following sampling period finishes and data reception begins.

In order to reduce the preamble length without missing packets, the sub-sampling must be converted to a continuous sliding window. This can be done in existing hardware by reprogramming of the FPGA on the digital sampling circuit. It is complicated by the non-sequential method of sub-sampling, but is still possible with careful tracking of the sampling clock phase and careful management of sample addresses so that new samples can replace old equivalent samples to keep a continuous sliding sub-sampled window for analysis.

Reducing the preamble duration can significantly improve the multi-tag performance of the system. The current system has a preamble of 270μS which using equation (3.5) has an ideal performance of 3704. If the ideal preamble duration of 149μS can be used, the ideal performance is 6711. This indicates that reducing the preamble duration can almost double the multi-tag performance.

6.3 Small Inexpensive Low Power Integrated Tag

The current proof-of-concept tag design utilizes discrete components and an FPGA as seen in figure 6.1. It is too large and spread out to be moved about during testing, too power hungry for battery operation, and the use of an FPGA makes it costly. An integrated tag design is needed that is small and self contained. The FPGA can be replaced by an inexpensive, low cost micro controller such as a Piccolo series micro controller from Texas Instruments. The transmitter can be integrated into a much smaller size board as done for the second generation integrated tag. Fabrication of integrated tags would help with future dynamic testing of tags, and would allow the creation of additional tags for larger scale multi-tag testing.

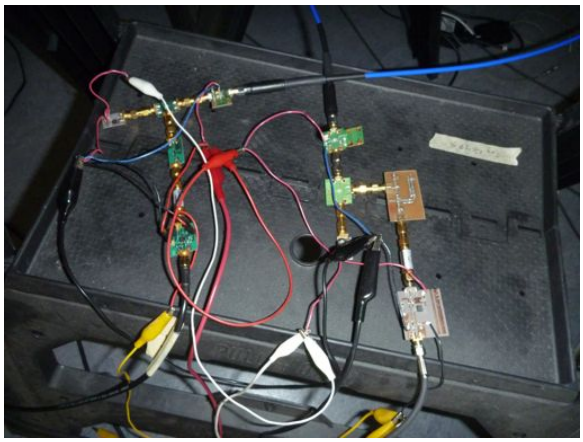

Figure 6.1: Tag constructed of discrete components for proof-of-concept work.

Chapter 7

Conclusion

The research described in this thesis offers a novel approach to multi-tag access for a high accuracy localization system based on utilizing the UWB radio for both localization and digital communication. This approach offers improvements in multi-tag performance by reducing the localization time required for individual tags. It also has the benefit of eliminating the need for a narrow band 2.4 GHz transceiver previously used in the second generation system. This work was motivated by the potential need of users to operate many collocated tags while maintaining the high update rates necessary to maintain millimeter position accuracy of moving objects.

This proof-of-concept system compares well with the previous 2nd generation UT system in terms of both localization accuracy and multi-tag performance, and advances the UT high accuracy localization system a step closer to matching the multi-tag performance of lower accuracy commercial systems. Table 7.1 compares the performance of both the commercial systems and 2nd generation UT high accuracy experimental system. It is challenging for a high accuracy localization system based on sub-sampling to match a lower accuracy system in multi-tag performance simply because of the additional time required to do sub-sampling based localization.

The use of UWB for both localization and communication has significant advantages over the pervious 2.4 GHz based communication system in many

Table 7.1: Comparison of both commercial and experimental systems.

System	Multi-tag Performance (EPS)	Localization Accuracy (mm)
Commercial Systems		
Zebra	3500	300
Ubisense	134	150
Time Domain	280	70
Decawave	11000	10
UT 2nd Generation	587.7	3.72
This Work	**889.1**	**3.25**

applications, but some advantages of using 2.4 GHz exist that may apply in specific applications. Table 7.2the additional pros and cons that exist for using either UWB or 2.4 GHz based multi-tag methods.

The final result of this work would not have been possible without the contributions of my advisor, other students, and past graduates whose work laid the foundation for this thesis. My individual contributions are toward the multi-tag access scheme and related system improvements. My contributions and the resulting system improvements are summarized in table 7.3.

The system developed through this work represents only an initial proof-of-concept design. Significant potential exists for continued system improvements both in multi-tag performance and localization accuracy based on the scheme developed here. A number of areas for potential optimization and future research spanning a range of disciplines are indicating by this research. Primary goals for future work include expansion of the system to 3-d dynamic tracking, improved multi-tag performance by better separating and recovering from frame collisions, and improved localization through improved digital signal processing. Further work in this field will be driven by the continuing goal of sub-millimeter accuracy with high multi-tag performance.

Table 7.2: Advantages and disadvantages of both the UWB and 2.4GHz based multi-tag access approach

2.4 GHz based multi-tag
Advantages
Wireless Tag Control
Synchronized tag transmission eliminates inter-tag interference
Commercially available development tools
Disadvantages
Requires a 2.4 GHz transceiver for each tag
Higher tag cost, increased power consumption, and complexity
Both UWB and Narrow Band signals
UWB based multi-tag
Advantages
Based on existing UWB transmitter
Lower tag cost and complexity
Single wireless channel (no narrow band)
Disadvantages
Transmit-only tag operation prevents wireless tag control
Currently no commercial off-the-shelf development tools
Asynchronous operation results in some probability of inter-tag interference

Table 7.3: My contributions and the resulting improvements in system performance.

Task	Resulting System Improvement
Developed figure of merit for comparing multi-tag performance	Allows easy comparison of multi-tag performance between systems utilizing differing number of tags and refresh rates
Integration of an FPGA based digital sampler with TDOA processing onboard	The digital sub-sampling scheme allows complete localization measurements to be made 7.5 times faster than the analog predecessor
Implementation of UWB OOK digital communications scheme	Allows successful transmission of 16 bit tag-ids using the UWB radio with a data rate of 10 Mbit per second
Implementation of multi-tag access high accuracy localization system	Maintains comparable localization accuracy while improving the multi-tag performance by more than 50% while eliminating the need for a narrowband control channel.
Experimental Analysis	Demonstrates favorable performance against the 2nd generation system in 1-D proof-of-concept system

Bibliography

[1] Zebra. (2011, November) Dart uwb hub and sensors. [Online]. Available: http://www.zebra.com/id/zebra/na/en/documentlibrary/product_brochures/dart_sensors.html viii, ix, 8, 9, 10

[2] Ubisense. (2011, November) Ubisense research package. [Online]. Available: http://www.ubisense.net/en/resources/factsheets/ubisense-research-package.html viii, ix, 8, 9

[3] ——. (2011, November) Real time location fact sheet. [Online]. Available: http://www.ubisense.net/en/media/pdfs/factsheets_pdf/48354_real-time-location-en090908.pdf viii, 8

[4] Time Domain. (2011, November) Pulson 400 data sheet. [Online]. Available: http://www.timedomain.com/datasheets/TD_DS_P400_RCM_11-7-11.pdf viii, ix, 8, 10

[5] DecaWave, "Scensor–precision location ultra low power transceiver," DecaWave, Advanced Product Information D0801004DS7, 2011. viii, ix, 8, 10

[6] M. Kuhn, M. Mahfouz, J. Turnmire, Y. Wang, and A. Fathy, "A multi-tag access scheme for indoor uwb localization systems used in medical environments," in *Biomedical Wireless Technologies, Networks, and Sensing Systems (BioWireleSS), 2011 IEEE Topical Conference on*, jan. 2011, pp. 75 –78. viii, 10, 43

[7] M. Kuhn, "Development and experimental analysis of wireless high accuracy ultra-wideband localization systems for indoor medical applications," Ph.D. dissertation, University of Tennesseee, May 2012. viii, ix, 7, 10, 11, 13, 14, 15, 16, 27

[8] Q. Liu, Y. Wang, and A. Fathy, "A compact integrated 100 gs/s sampling module for uwb see through wall radar with fast refresh rate for dynamic real time imaging," in *Radio and Wireless Symposium (RWS), 2012 IEEE*, jan. 2012, pp. 59 –62. 3

[9] C. Copps and Martin, "Revision of part 15 of the commission's rules regarding ultra-wideband transmission," Federal Communications Commission First Report and Order, April 2002. 5

[10] H. Liu, H. Darabi, P. Banerjee, , and J. Liu, "Survey of wireless indoor positioning techniques and systems," *IEEE Transactions On Systems, Man, and Cybernetics*, vol. 37, no. 6, pp. 1067–1080, November 2007. 6

[11] IEEE, *IEEE 802.15.4a Standard for Information technology— Telecommunications and information exchange between systems— Local and metropolitan area networks–Wireless Medium Access Control (MAC) and Physical Layer (PHY) Specifications for Low-Rate Wireless Personal Area Networks (WPANs).* pub-IEEE-STD, 2007. 6, 7

[12] C. Zhang and A. Fathy, "Reconfigurable pico-pulse generator for uwb applications," in *Microwave Symposium Digest, 2006. IEEE MTT-S International*, june 2006, pp. 407 –410. 11, 44

[13] H. C. Keong and M. R. Yuce, "Analysis of a multi-access and asynchronous transmit-only uwb for wireless body area networks," in *31st Annual International Conference of the IEEE Engineering in Medicine and Biology Society*, September 2009, pp. 6906–6909. 28, 29

[14] C. Y. Jung, J. W. Chong, Y. J. Hong, B. C. Jung, and D. K. Sung, "Orthogonal time hopping multiple access for uwb impulse radio communications," in *Asia-Pacific Conference on Communications*, October 2005. 29, 30, 31

[15] Xilinx, "Logicore ip clocking wizard v1.8," Xilinx, Product Specification DS709, 2010. 41

[16] P. Alfke, "Efficient shift registers, lfsr counters, and long pseudo-random sequence generators," Xilinx, Application Note XAPP 052, July 1996. 42

[17] M. Leib, T. Mach, B. Schleicher, C. Ulusoy, W. Menzel, and H. Schumacher, "Demonstration of uwb communication for implants using an energy detector," in *German Microwave Conference*, July 2010, pp. 158–161. 45

[18] "http://www.ndigital.com/lifesciences/certus-techspecs.php." 51

Vita

Nathan Carl Rowe is a graduate of The University of Tennessee where he received his B.S. in Electrical Engineering with a focus on communications technology in 2008, and a M.S. in Electrical Engineering with a concentration in Microwave Circuits in 2012. He is currently a research and development engineer in the Global Nuclear Security Technology Division at the Oak Ridge National Laboratory where he began working in 2009. He is a 2010 fellow of the World Nuclear University and founding member of the Next Generation Safeguards Professionals Network. He has authored and coauthored numerous conference papers for the Institute of Nuclear Materials Management (INMM) annual meeting, and coauthored a recent Journal of Nuclear Materials Management paper. He has been an active member of the INMM since 2011 and a member of the Institute of Electrical and Electronics Engineers (IEEE) since 2007.

Mr. Rowe's work experience includes a broad range of nuclear nonproliferation and nuclear security areas including item tagging and tracking, tamper indicating devices for containment and surveillance, radiation portal monitor systems for detecting illicit trafficking in radioactive material, and physical security technologies including systems for border security. He has experience in hardware and software development along with systems level design and evaluation. His current research interests include security issues and solutions for wireless tagging and tracking systems, ultra-wideband systems for communication and localization, and technologies and techniques for improved tamper detection in remotely monitored systems.